WG1 meeting

Swansea, 12-14 September 2017

Maria Paola Lombardo
INFN

Topology and axions' dark matter from lattice QCD at high T

QCD topology, long standing focus of strong interaction:

-learning about:
 the structure of the (s)QGP
 fundamental symmetries, η'mass, strongCP problem —> axions

-hampered by technical difficulties

Recent developments:
-methodological progress: gradient flow, chiral fermions
-first results for dynamical fermions at high temperature:

Trunin *et al.* **J.Phys.Conf.Ser. 668 (2016) no.1, 012123**
Bonati *et al.* **JHEP 1603 (2016) 155**
Borsany *et al.* **Nature 539 (2016) no.7627, 69-71**
Petreczky *et al.* **Phys.Lett. B762 (2016) 498-505**
Burger *et al.* **Nucl. Phys. A, in press**
Taniguchi *et al.* **Phys.Rev. D95 (2017) no.5, 054502**

TmFT

+work in progress

Pseudoscalar spectrum, and η' / UA(1) puzzle

Particle name	Particle symbol	Antiparticle symbol	Quark content	Rest mass (MeV/c²)
Pion[6]	π^+	π^-	$u\bar{d}$	139.570 18 ±0.000 35
Pion[7]	π^0	Self	$\frac{u\bar{u}-d\bar{d}}{\sqrt{2}}$ [a]	134.9766 ±0.0006
Eta meson[8]	η	Self	$\frac{u\bar{u}+d\bar{d}-2s\bar{s}}{\sqrt{6}}$ [a]	547.862 ±0.018
Eta prime meson[9]	η'(958)	Self	$\frac{u\bar{u}+d\bar{d}+s\bar{s}}{\sqrt{3}}$ [a]	957.78 ±0.06
Kaon[12]	K^+	K^-	$u\bar{s}$	493.677 ±0.016
Kaon[13]	K^0	$\bar{K}^0$	$d\bar{s}$	497.614 ±0.024

η' and the $U_A(1)$ problem:

$U_A(1)$ symmetry $q \to e^{i\alpha\gamma_5} q$

Would be broken by the (spontaneously generated) $\bar{q}q$:

the candidate Goldstone is the η'
Heavy!! (900 MeV)

BUT:
the divergence of the current $j_5^\mu = \bar{q}\gamma_5\gamma_\mu q,$

$$\partial_\mu j_5^\mu = m\bar{q}\gamma_5 q + \frac{1}{32\pi^2} F\tilde{F}.$$

Contains another term

Particle name	Particle symbol	Antiparticle symbol	Quark content	Rest mass (MeV/c^2)
Pion[6]	π^+	π^-	$u\bar{d}$	139.570 18 ±0.000 35
Pion[7]	π^0	Self	$\frac{u\bar{u}-d\bar{d}}{\sqrt{2}}$ [a]	134.9766 ±0.0006
Eta meson[8]	η	Self	$\frac{u\bar{u}+d\bar{d}-2s\bar{s}}{\sqrt{6}}$ [a]	547.862 ±0.018
Eta prime meson[9]	η'(958)	Self	$\frac{u\bar{u}+d\bar{d}+s\bar{s}}{\sqrt{3}}$ [a]	957.78 ±0.06
Kaon[12]	K^+	K^-	$u\bar{s}$	493.677 ±0.016
Kaon[13]	K^0	$\bar{K}^0$	$d\bar{s}$	497.614 ±0.024

The $U_A(1)$ symmetry is explicit broken

....

The θ dependence solves the $U_A(1)$ problem: ......provided that

$$\frac{1}{32\pi^2}\int d^4x F\tilde{F}$$

is different from zero.

It can be proven that $\frac{1}{32\pi^2}\int d^4x F\tilde{F}$ = Q (topological charge)

and

$$Q = n_+ - n_-$$

……provided that

$$\frac{1}{32\pi^2}\int d^4x F\tilde{F}$$

is different from zero.

It can be proven that

$$\frac{1}{32\pi^2}\int d^4x F\tilde{F} = Q$$

Gluonic definition

and

$$Q = n_+ - n_-$$

Fermionic definition

The η' mass may now be computed from the decay of the correlation

$$\langle \partial_\mu j_5^\mu(x) \partial_\mu j_5^\mu(y) \rangle \propto \frac{1}{N^2} \langle F(x)\tilde{F}(x) F(y)\tilde{F}(y) \rangle$$

which at leading order gives the Witten-Veneziano formula

$$m_{\eta'}^2 = \frac{2N_f}{F_\pi^2}\chi_t^{\mathrm{qu}}$$

Lattice studies of η, η'

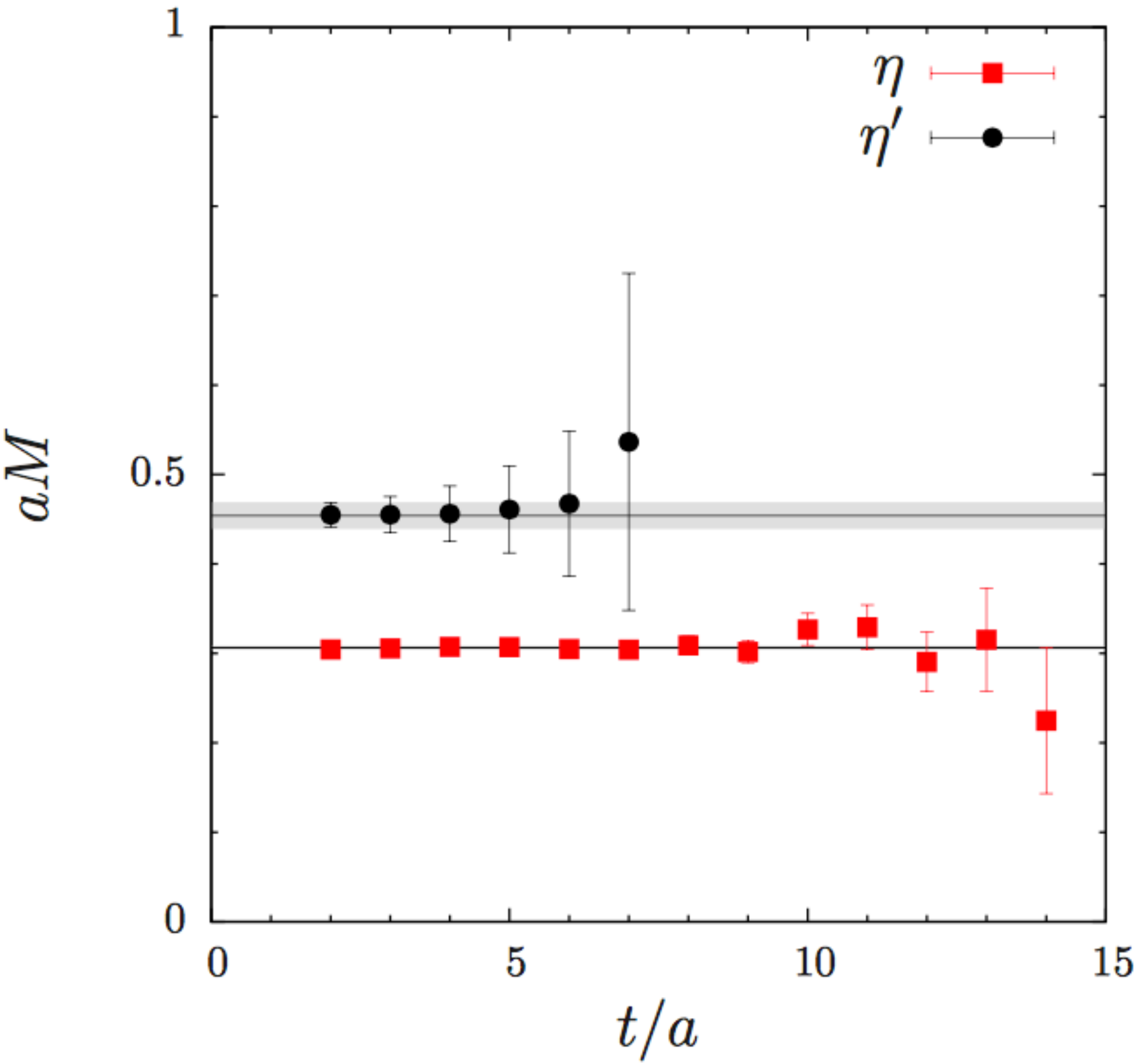

Otnnad, Urbach, Michael (ETMC)
2013

$$M_\eta = 551(8)_{\rm stat}(6)_{\rm sys}\,.$$

$$M_{\eta'} = 1006(54)_{\rm stat}(38)_{\rm sys}(+61)_{\rm ex}$$

OK!

A θ term solves the $U_A(1)$ problem

$$\mathcal{L}_{QCD}(\theta) = \mathcal{L}_{QCD} + \frac{g^2\theta}{32\pi^2}\epsilon^{\mu\nu\rho\sigma}F^a_{\mu\nu}F^a_{\rho\sigma}.$$

$$Q = \int d^4x \, \frac{g^2}{32\pi^2}\mathrm{tr}F\tilde{F}$$

θ term solves $U_A(1)$ problem

$$\mathcal{L}_{QCD}(\theta) = \mathcal{L}_{QCD} + \frac{g^2\theta}{32\pi^2}\epsilon^{\mu\nu\rho\sigma}F^a_{\mu\nu}F^a_{\rho\sigma}.$$

Ammitted but $\theta < 10^{-9}$

$$Q = \int d^4x \, \frac{g^2}{32\pi^2}\mathrm{tr}F\tilde{F}$$

but: it poses a naturalness issue … (more later)…

θ term solves $U_A(1)$ problem

$$\mathcal{L}_{QCD}(\theta) = \mathcal{L}_{QCD} + \frac{g^2\theta}{32\pi^2}\epsilon^{\mu\nu\rho\sigma}F^a_{\mu\nu}F^a_{\rho\sigma}.$$

Ammitted but $\theta < 10^{-9}$

$$Q = \int d^4x \, \frac{g^2}{32\pi^2}\mathrm{tr}F\tilde{F}$$

We then consider:

$$Z_{QCD}(\theta, T) = \int [dA][d\psi][d\bar{\psi}] \exp\left(-T\sum_t d^3x \, \mathcal{L}_{QCD}(\theta)\right) = \exp[-VF(\theta, T)]$$

A note on computation:

$$\mathcal{L}_{QCD}(\theta) = \mathcal{L}_{QCD} + \frac{g^2\theta}{32\pi^2}\epsilon^{\mu\nu\rho\sigma}F^a_{\mu\nu}F^a_{\rho\sigma}.$$

Ammitted but $\theta < 10^{-9}$

$$Q = \int d^4x \, \frac{g^2}{32\pi^2}\mathrm{tr}F\tilde{F}$$

Sign problem

Approach similar in spirit to Taylor expansion for chempot

$$Z_{QCD}(\theta,T) = \int [dA][d\psi][d\bar{\psi}] \exp\left(-T\sum_t d^3x \, \mathcal{L}_{QCD}(\theta)\right) = \exp[-VF(\theta,T)$$

Simulations at $\theta = 0$

$$\left.\frac{\partial^2 F(\theta,T)}{\partial\theta^2}\right|_{\theta=0} \equiv \chi(T), = (< Q^2 > - < Q >^2)/V$$

Comparison of topological charge definitions in Lattice QCD

Constantia Alexandrou[a,b], Andreas Athenodorou[b,a], Krzysztof Cichy[c,d], Arthur Dromard[e], Elena Garcia-Ramos[f,g], Karl Jansen[f], Urs Wenger[h], Falk Zimmermann[i]

2017

Comparison of topological charge definitions

nr	full name	smearing type	short name	type
1	index of overlap Dirac operator $s = 0.4$	–	index nonSmear $s = 0.4$	F
2	index of overlap Dirac operator $s = 0.0$	–	index nonSmear $s = 0$	F
3	index of overlap Dirac operator $s = 0.0$	HYP1	index HYP1 $s = 0$	F
4	Wilson-Dirac op. spectral flow $s = 0.0$	HYP1	SF HYP1 $s = 0.0$	F
5	Wilson-Dirac op. spectral flow $s = 0.75$	HYP1	SF HYP1 $s = 0.75$	F
6	Wilson-Dirac op. spectral flow $s = 0.0$	HYP5	SF HYP5 $s = 0.0$	F
7	Wilson-Dirac op. spectral flow $s = 0.5$	HYP5	SF HYP5 $s = 0.5$	F
8	spectral projectors $M^2 = 0.00003555$	–	spec. proj. $M^2 = 0.0000355$	F
9	spectral projectors $M^2 = 0.0004$	–	spec. proj. $M^2 = 0.0004$	F
10	spectral projectors $M^2 = 0.0010$	–	spec. proj. $M^2 = 0.0010$	F
11	spectral projectors $M^2 = 0.0015$	–	spec. proj. $M^2 = 0.0015$	F
12	field theoretic (clover)	–	cFT nonSmear	G
13	field theoretic (plaquette)	GF (Wplaq,t_0)	pFT GF Wplaq t_0	G
14	field theoretic (plaquette)	GF (Wplaq,$2t_0$)	pFT GF Wplaq $2t_0$	G
15	field theoretic (plaquette)	GF (Wplaq,$3t_0$)	pFT GF Wplaq $3t_0$	G
16	field theoretic (clover)	GF (Wplaq,t_0)	cFT GF Wplaq t_0	G
17	field theoretic (clover)	GF (Wplaq,$2t_0$)	cFT GF Wplaq $2t_0$	G
18	field theoretic (clover)	GF (Wplaq,$3t_0$)	cFT GF Wplaq $3t_0$	G
19	field theoretic (improved)	GF (Wplaq,t_0)	iFT GF Wplaq t_0	G
20	field theoretic (improved)	GF (Wplaq,$2t_0$)	iFT GF Wplaq $2t_0$	G
21	field theoretic (improved)	GF (Wplaq,$3t_0$)	iFT GF Wplaq $3t_0$	G
22	field theoretic (clover)	GF (tlSym,t_0)	cFT GF tlSym t_0	G
23	field theoretic (clover)	GF (tlSym,$2t_0$)	cFT GF tlSym $2t_0$	G
24	field theoretic (clover)	GF (tlSym,$3t_0$)	cFT GF tlSym $3t_0$	G
25	field theoretic (clover)	GF (Iwa,t_0)	cFT GF Iwa t_0	G
26	field theoretic (clover)	GF (Iwa,$2t_0$)	cFT GF Iwa $2t_0$	G
27	field theoretic (clover)	GF (Iwa,$3t_0$)	cFT GF Iwa $3t_0$	G
28	field theoretic (clover)	cool (Wplaq,t_0)	cFT cool (GF Wplaq t_0)	G
29	field theoretic (clover)	cool (Wplaq,$3t_0$)	cFT cool (GF Wplaq $3t_0$)	G
30	field theoretic (clover)	cool (tlSym,t_0)	cFT cool (GF tlSym t_0)	G
31	field theoretic (clover)	cool (tlSym,$3t_0$)	cFT cool (GF tlSym $3t_0$)	G
32	field theoretic (clover)	cool (Iwa,t_0)	cFT cool (GF Iwa t_0)	G
33	field theoretic (clover)	cool (Iwa,$3t_0$)	cFT cool (GF Iwa $3t_0$)	G
34	field theoretic (clover)	stout (0.01,t_0)	cFT stout 0.01 (GF Wplaq t_0)	G
35	field theoretic (clover)	stout (0.01,$3t_0$)	cFT stout 0.01 (GF Wplaq $3t_0$)	G
36	field theoretic (clover)	stout (0.1,t_0)	cFT stout 0.1 (GF Wplaq t_0)	G
37	field theoretic (clover)	stout (0.1,$3t_0$)	cFT stout 0.1 (GF Wplaq $3t_0$)	G
38	field theoretic (clover)	APE (0.4,t_0)	cFT APE 0.4 (GF Wplaq t_0)	G
39	field theoretic (clover)	APE (0.4,$3t_0$)	cFT APE 0.4 (GF Wplaq $3t_0$)	G
40	field theoretic (clover)	APE (0.5,t_0)	cFT APE 0.5 (GF Wplaq t_0)	G
41	field theoretic (clover)	APE (0.5,$3t_0$)	cFT APE 0.5 (GF Wplaq $3t_0$)	G
42	field theoretic (clover)	APE (0.6,t_0)	cFT APE 0.6 (GF Wplaq t_0)	G
43	field theoretic (clover)	APE (0.6,$3t_0$)	cFT APE 0.6 (GF Wplaq $3t_0$)	G
44	field theoretic (clover)	HYP (t_0)	cFT HYP (GF Wplaq t_0)	G
45	field theoretic (clover)	HYP ($3t_0$)	cFT HYP (GF Wplaq $3t_0$)	G

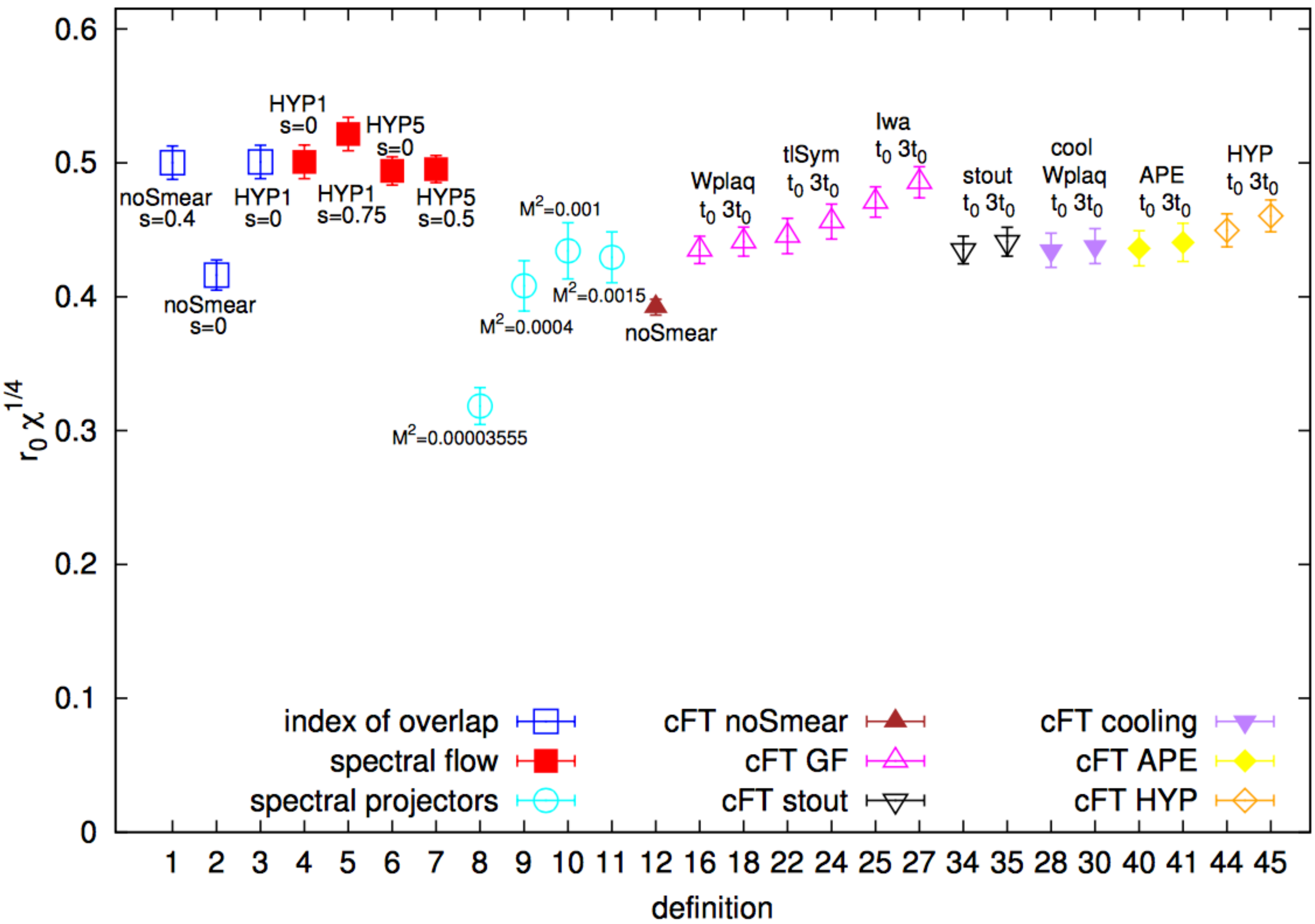

r_0 χ^1/4
definition
0.6
0.5
0.4
0.3
0.2
0.1
0
1 2 3 4 5 6 7 8 9 10 11 12 16 18 22 24 25 27 34 35 28 30 40 41 44 45
noSmear s=0.4
noSmear s=0
HYP1 s=0
HYP1 s=0
HYP5 s=0
HYP1 s=0.75
HYP5 s=0.5
M²=0.00003555
M²=0.0004
M²=0.001
M²=0.0015
noSmear
Wplaq t0 3t0
tlSym t0 3t0
Iwa t0 3t0
stout t0 3t0
cool Wplaq t0 3t0
APE t0 3t0
HYP t0 3t0
index of overlap
spectral flow
spectral projectors
cFT noSmear
cFT GF
cFT stout
cFT cooling
cFT APE
cFT HYP

T=0 results satisfactory

(of course there is room for improvement)

From now on:

High Temperature

The two faces of Hot QCD topology

Window to Axions

Property of Quark Gluon Plasma

Our setup at a glance

Hot QCD and Nf 2+1+1 twisted mass Wilson fermions

up,down
in the isospin limit

Physical strange

Physical charm

Why Nf = 2 +1 +1 ?

Tc

$\approx$200MeV

340 –380 MeV RHIC AuAu 200 GeV	420-480 MeV LHC 2.76 TeV	500- 600MeV LHC hot spots 2.76 TeV	→	1 GeV LHC 7 TeV

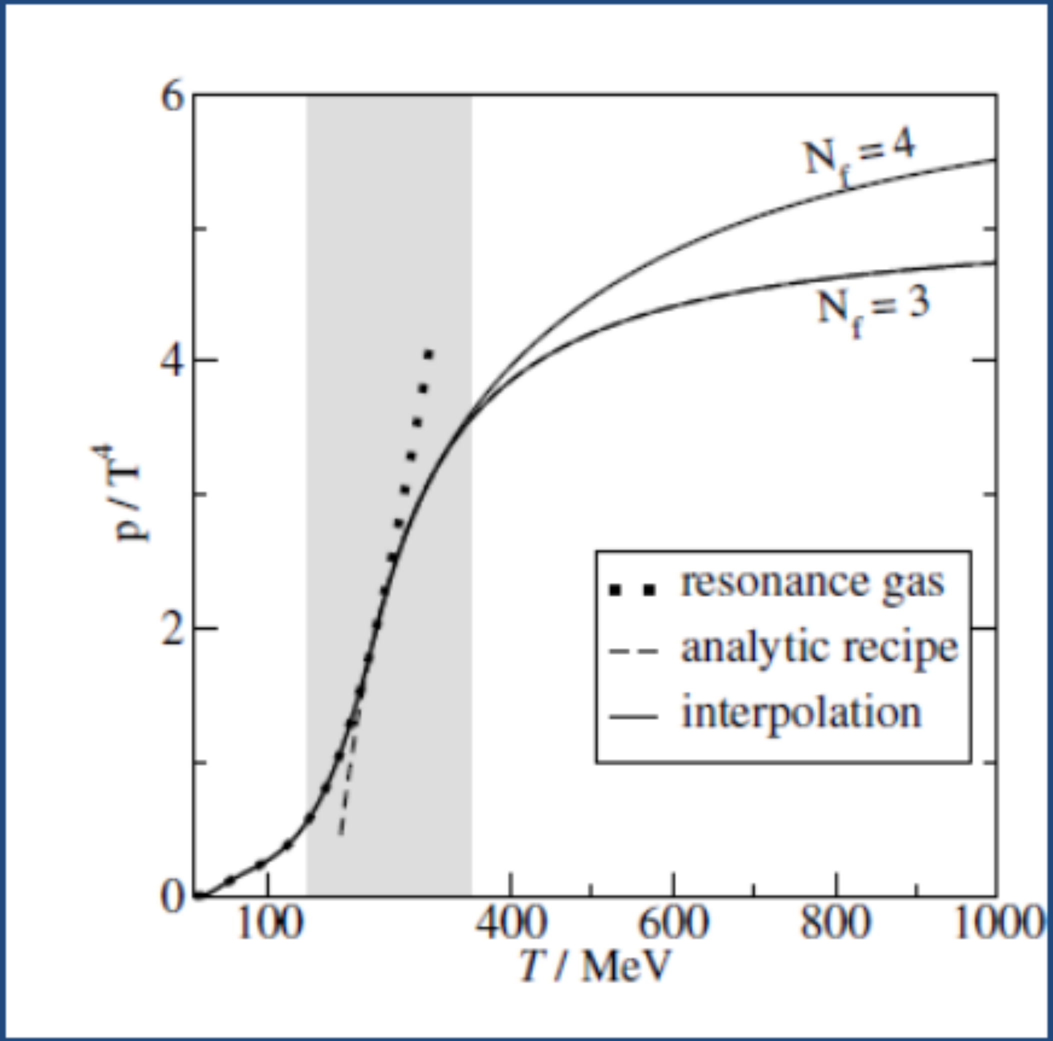

Quark Gluon Plasma @ Colliders

Analytic studies suggest that a dynamical charm becomes relevant above 400 MeV, well within the reach of LHC

Laine Schroeder 2006

Setup

Fixed varying scale

For each lattice spacing we explore a range of temperatures 150MeV — 500 MeV by varying Nt

We repeat this for three different lattice spacings following ETMC T=0 simulations.

Four pion masses

Number of flavours	$m_{\pi^\pm}$
$N_f = 2+1+1$	210
	260
	370
	470
$N_f = 2$	360
	430

Advantages: we rely on the setup of ETMC T=0 simulations. Scale is set once for all.

Disadvantages: mismatch of temperatures - need interpolation before taking the continuum limit

$T=0$ (ETMC) nomenclature	β	a [fm] [6]	N_σ^3	N_τ	T [MeV]	# confs.
A60.24	1.90	0.0936(38)	24^3	5	422(17)	585
				6	351(14)	1370
				7	301(12)	341
				8	263(11)	970
				9	234(10)	577
				10	211(9)	525
				11	192(8)	227
				12	176(7)	1052
			32^3	13	162(7)	294
				14	151(6)	1988
B55.32	1.95	0.0823(37)	32^3	5	479(22)	595
				6	400(18)	345
				7	342(15)	327
				8	300(13)	233
				9	266(12)	453
				10	240(11)	295
				11	218(10)	667
				12	200(9)	1102
				13	184(8)	308
				14	171(8)	1304
				15	160(7)	456
				16	150(7)	823
D45.32	2.10	0.0646(26)	32^3	6	509(20)	403
				7	436(18)	412
				8	382(15)	416
				10	305(12)	420
				12	255(10)	380
				14	218(9)	793
				16	191(8)	626
			40^3	18	170(7)	599
			48^3	20	153(6)	582

Results I

Gluonic (butterfly) operator

+

Gradient Flow Method

Q

$$\mathcal{L}_\theta = \frac{1}{4} F^a_{\mu\nu}(x) F^a_{\mu\nu}(x) - i\theta \boxed{\frac{g^2}{64\pi^2} \epsilon_{\mu\nu\rho\sigma} F^a_{\mu\nu}(x) F^a_{\rho\sigma}(x)},$$

$$\exp[-VF(\theta)] = \int [dA] \exp\left(-\int d^4x \mathcal{L}_\theta\right)$$

Gradient flow

Lüscher, Lüscher Weisz

Evolve the link variables in a fictitious flow time:

$$\dot{V}_{x,\mu}(t) = -g_0^2 \left[\partial_{x,\mu} S_{\text{Wilson}}(V(t)) \right] V_{x,\mu}(t),$$

Monitor $\langle E \rangle = \frac{1}{2 N_\tau N_\sigma^3} \sum_{x,\mu,\nu} \mathrm{Tr}[F_{\mu\nu}(x) F^{\mu\nu}(x)]$ as a function of t

Stop flowing when $t^2 \langle E \rangle \big|_{t=t_0} = 0.3$

Observables $< O(t) >$ renormalized at $\mu = 1/\sqrt{8t}$

Continuum limit of $< O(t) >$ is independent on the chosen reference value

Caveat: note comments by Kanaya et al.

Distribution of the topological charge *P(Q)*

cluster around integers as cooling proceeds

(results for a = 0.06 fm)

T=153 MeV

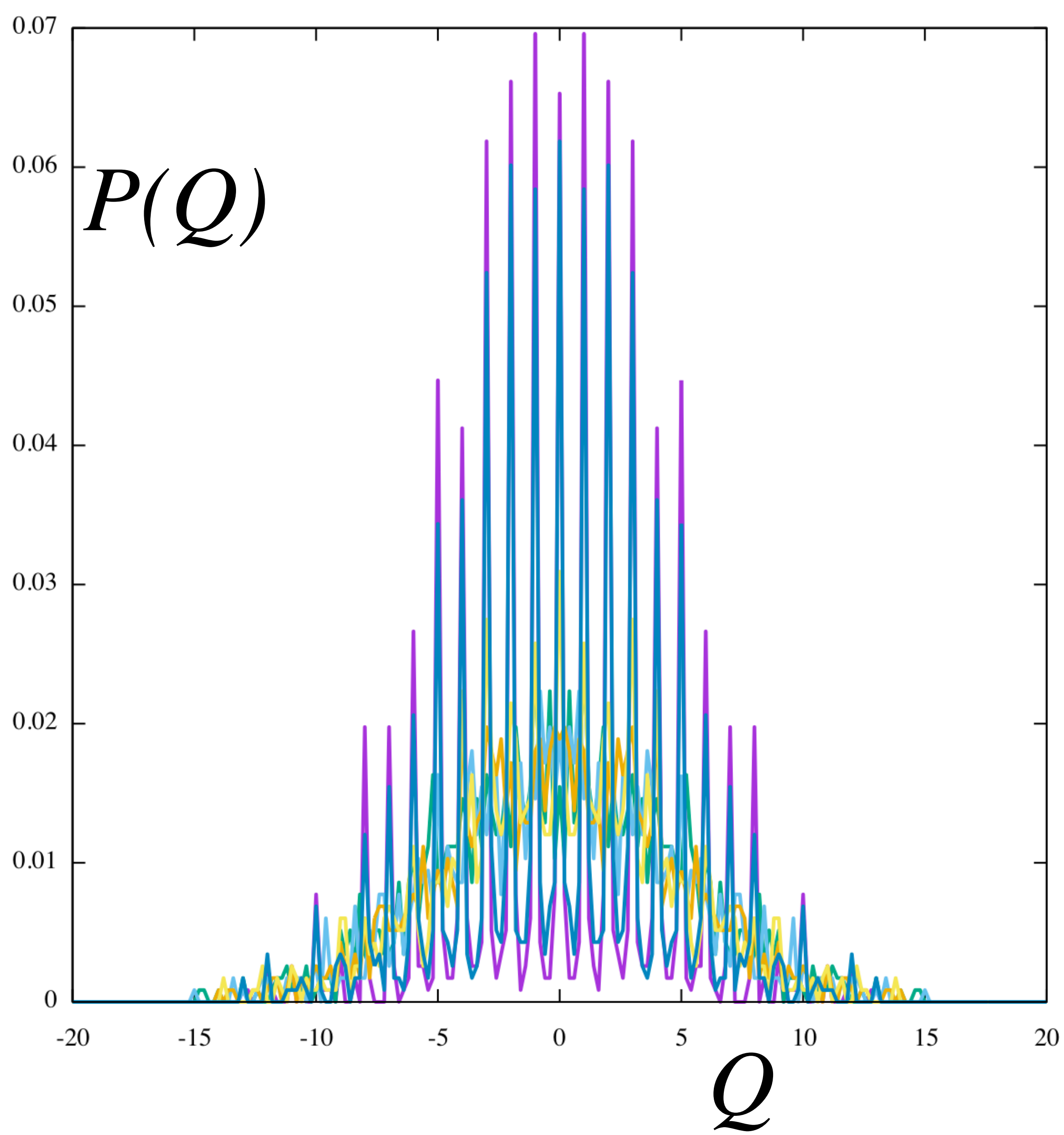

T=253 MeV

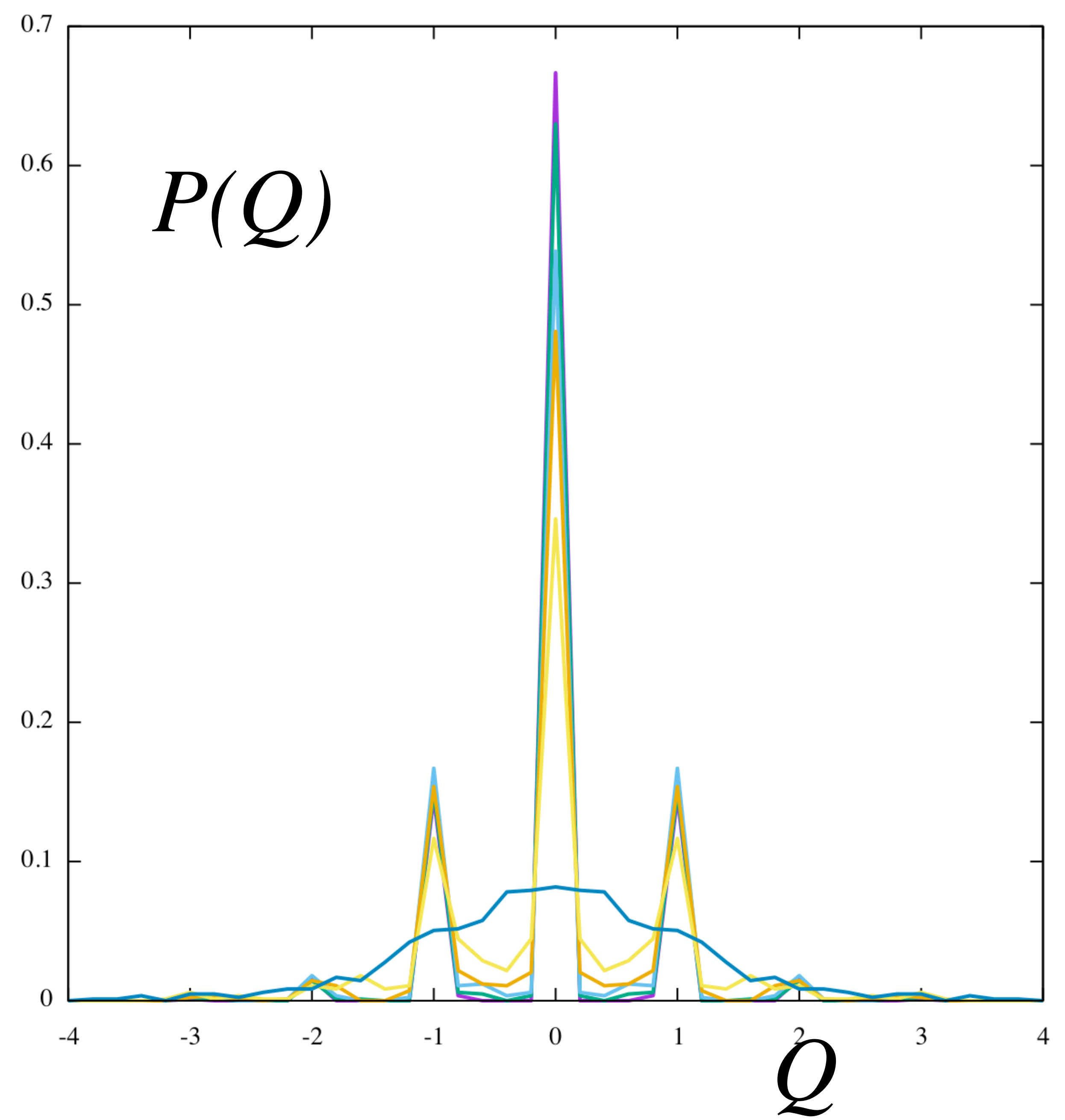

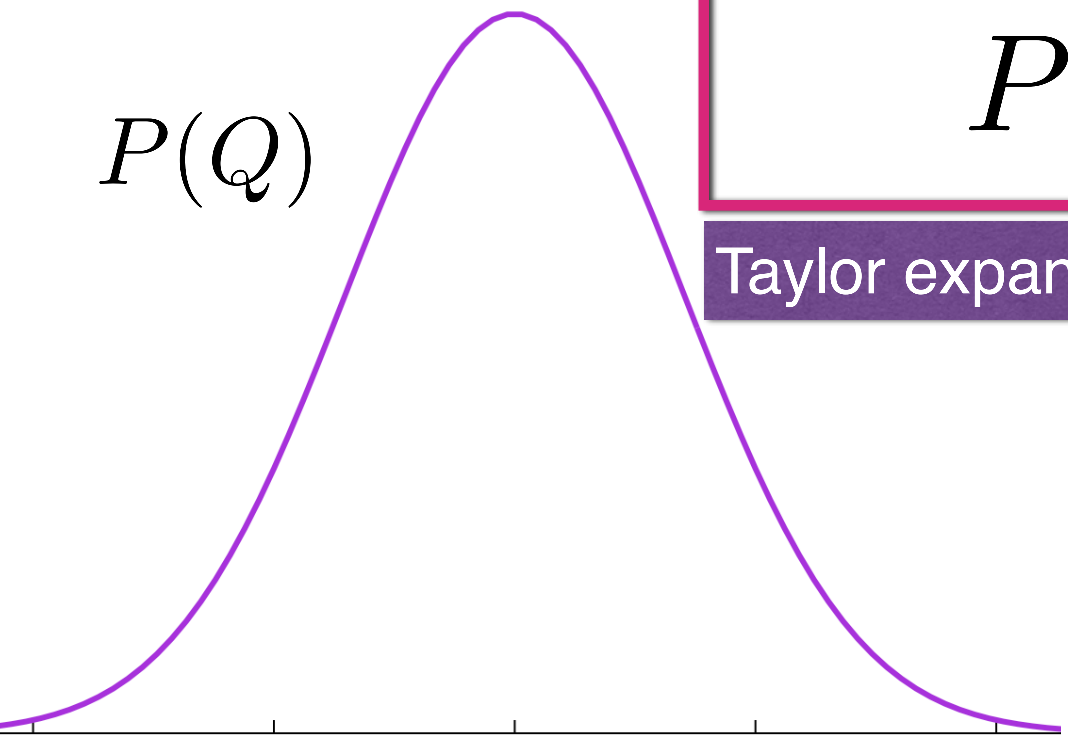

$P(Q)$ and $F(\theta)$

Taylor expansion, and cumulants of the topological charge distribution

$$e^{-F(\theta)} = \langle e^{i\theta Q} \rangle$$

$$P_\nu = \int_{-\pi}^{\pi} \frac{d\theta}{2\pi} e^{-i\theta\nu} e^{-F(\theta)} \qquad Q = \nu$$

$$C_n = (-1)^{n+1} \frac{1}{V} \frac{d^{2n}}{d\theta^{2n}} F(\theta)\Big|_{\theta=0} \equiv < Q^{2n} >_{conn}$$

$$F(\theta) = V \sum_{n=1}^{\infty} (-1)^{n+1} \frac{\theta^{2n}}{(2n)!} C_n$$

$$P_\nu = \frac{e^{-\frac{\nu^2}{2\sigma^2}}}{\sqrt{2\pi\sigma^2}} \left[1 + \frac{1}{4!} \frac{\tau}{\sigma^2} \mathrm{He}_4\left(\nu/\sigma\right) \right]$$

$\sigma^2 = V C_1$ and $\tau = C_2/C_1$ $\quad$ *P(Q)* is Gaussian for $V \to \infty$

$F(\theta)$ is ‘hidden’ in *P(Q)*’s cumulants

In practice only the first two cumulants are accessible:

$$F(\theta, T) = 1/2\chi(T)\theta^2 s(\theta, t)$$

$$s(\theta, T)1 + b_2(T)\theta^2 + \ldots$$

$$b_2 = -\frac{<Q^4>-3<Q^2>^2}{12<Q^2>}$$

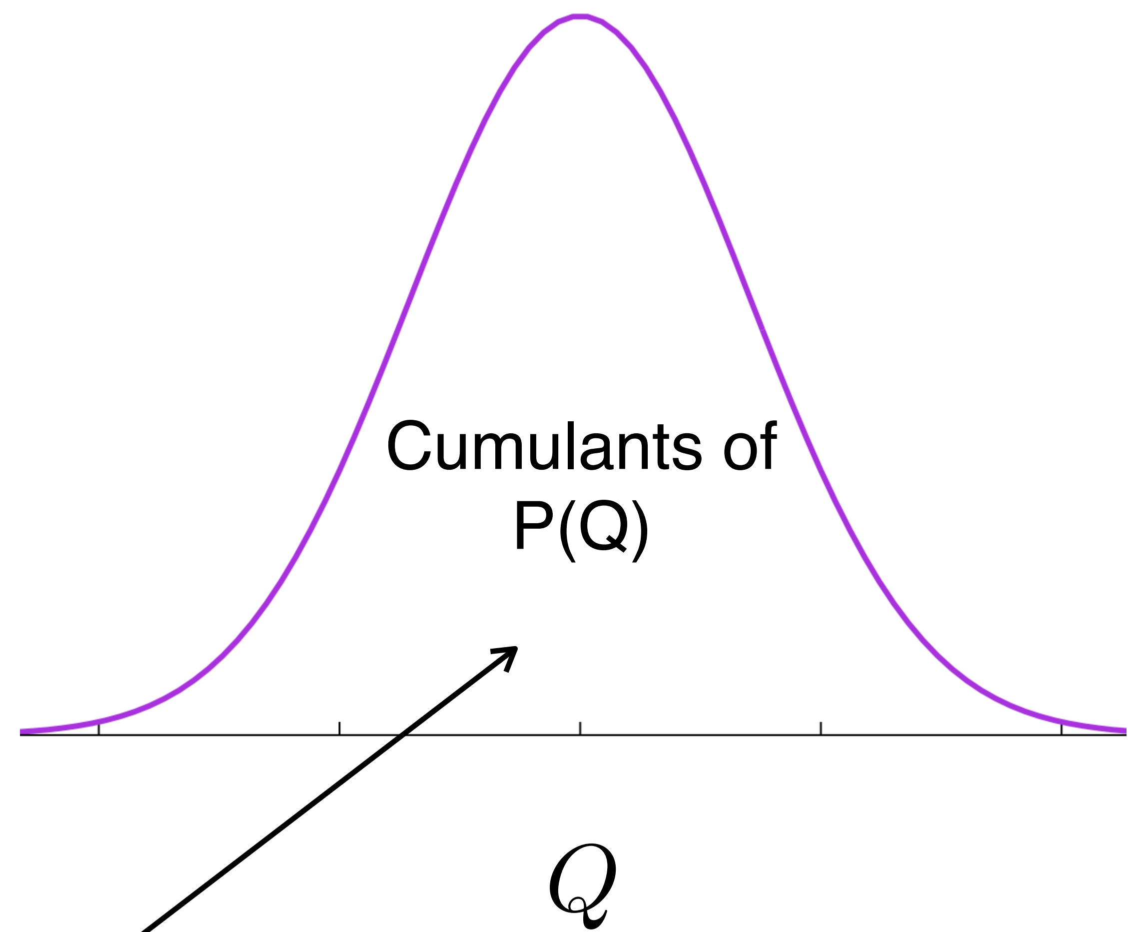

Taylor coefficients of $F(\theta, T)$

DIGA — at very high temperature — predicts

$$F(\theta, T) - F(0, T) = \chi(T)(1 - cos(\theta)) \longrightarrow b_2 = -1/12$$

Flowing towards the plateau

$$t^2 < E > |_{t=t_x, x=0-6} = (0.3, 0.66, 0.1, 0.15, 0.2, 0.25, 0.45)$$

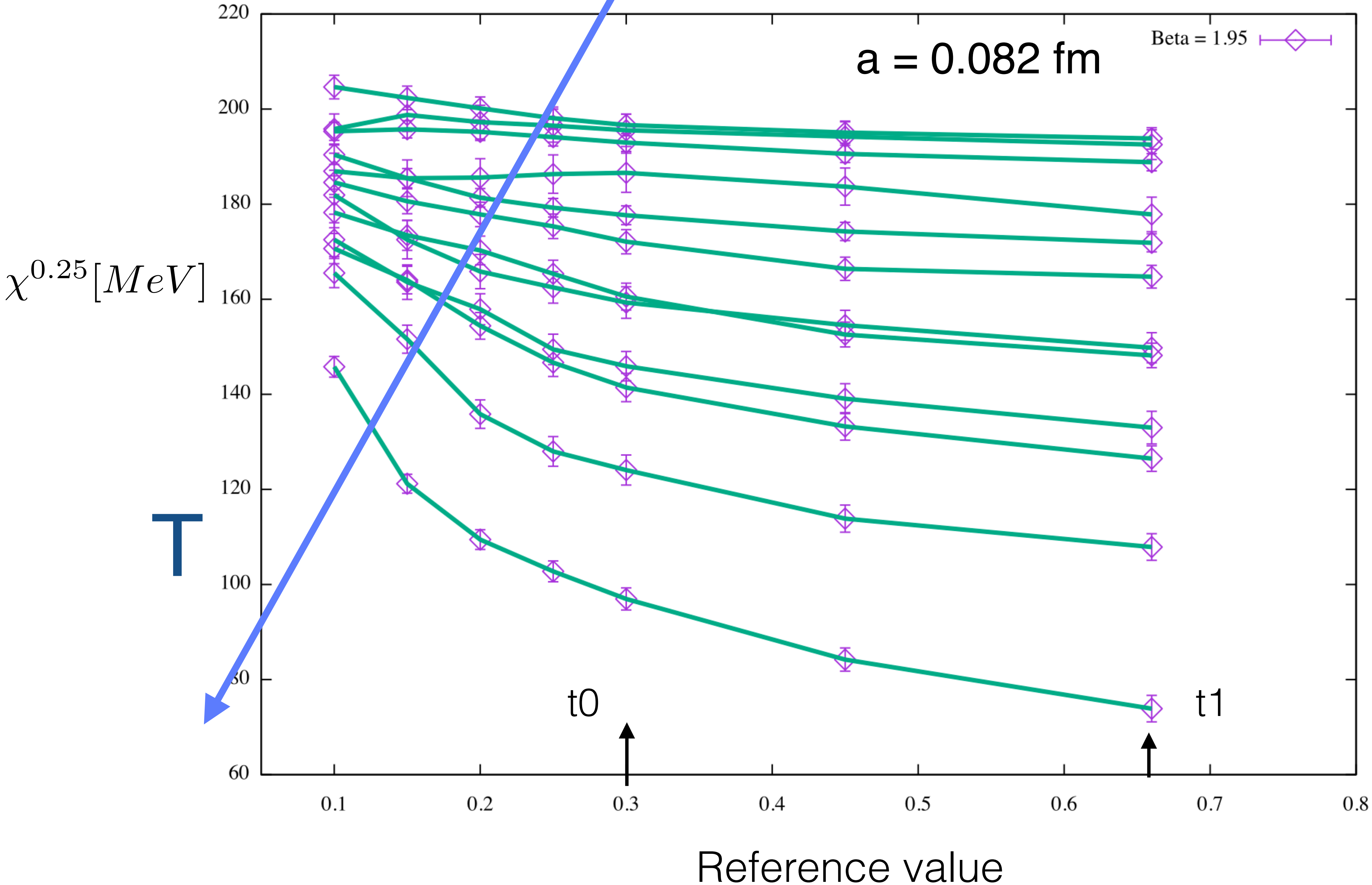

We focus on t(0.3) = t0 and t(0.66)= t1

On finer lattices, plateau is almost reached:

Gradient method coincides with cooling

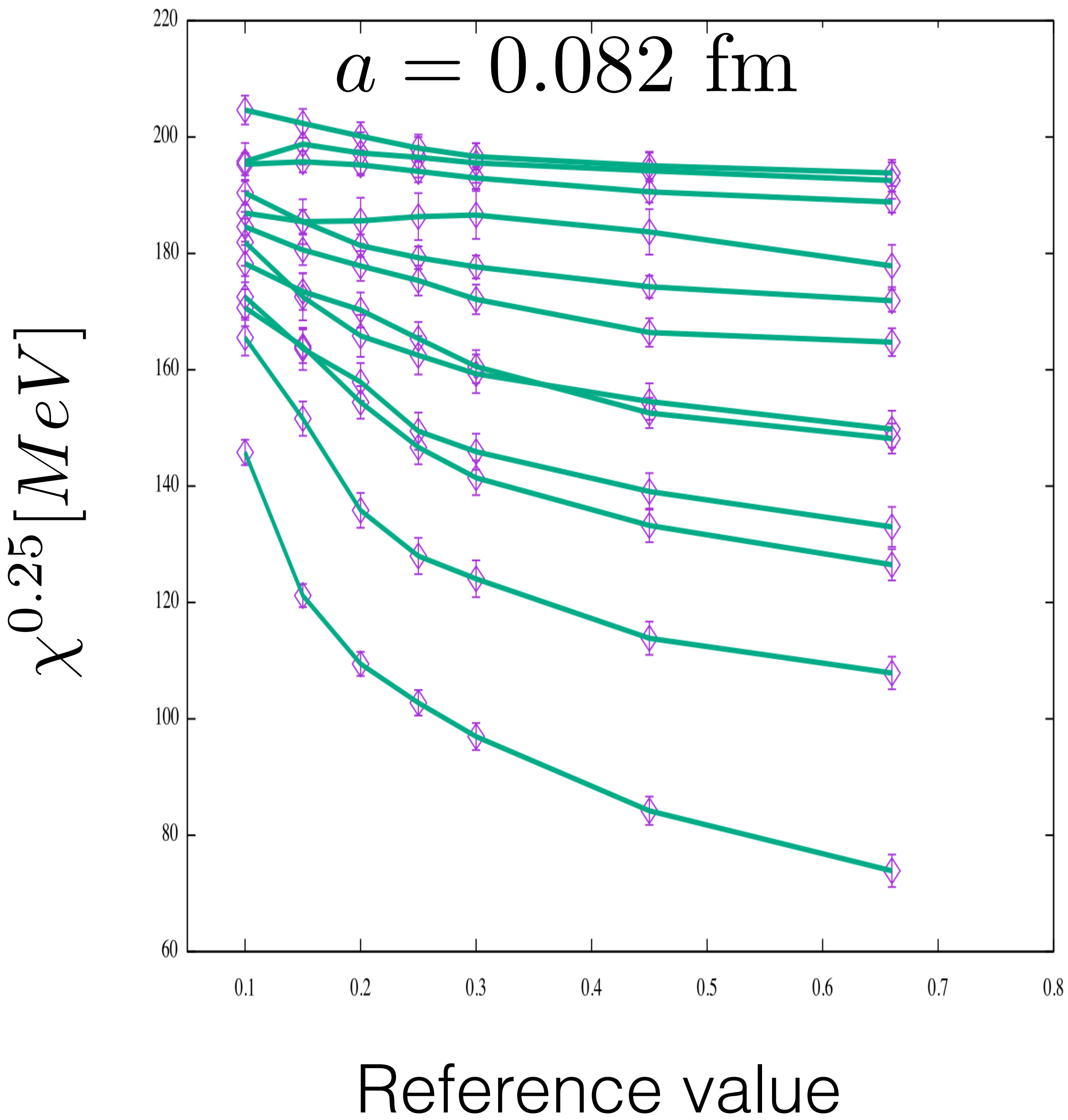

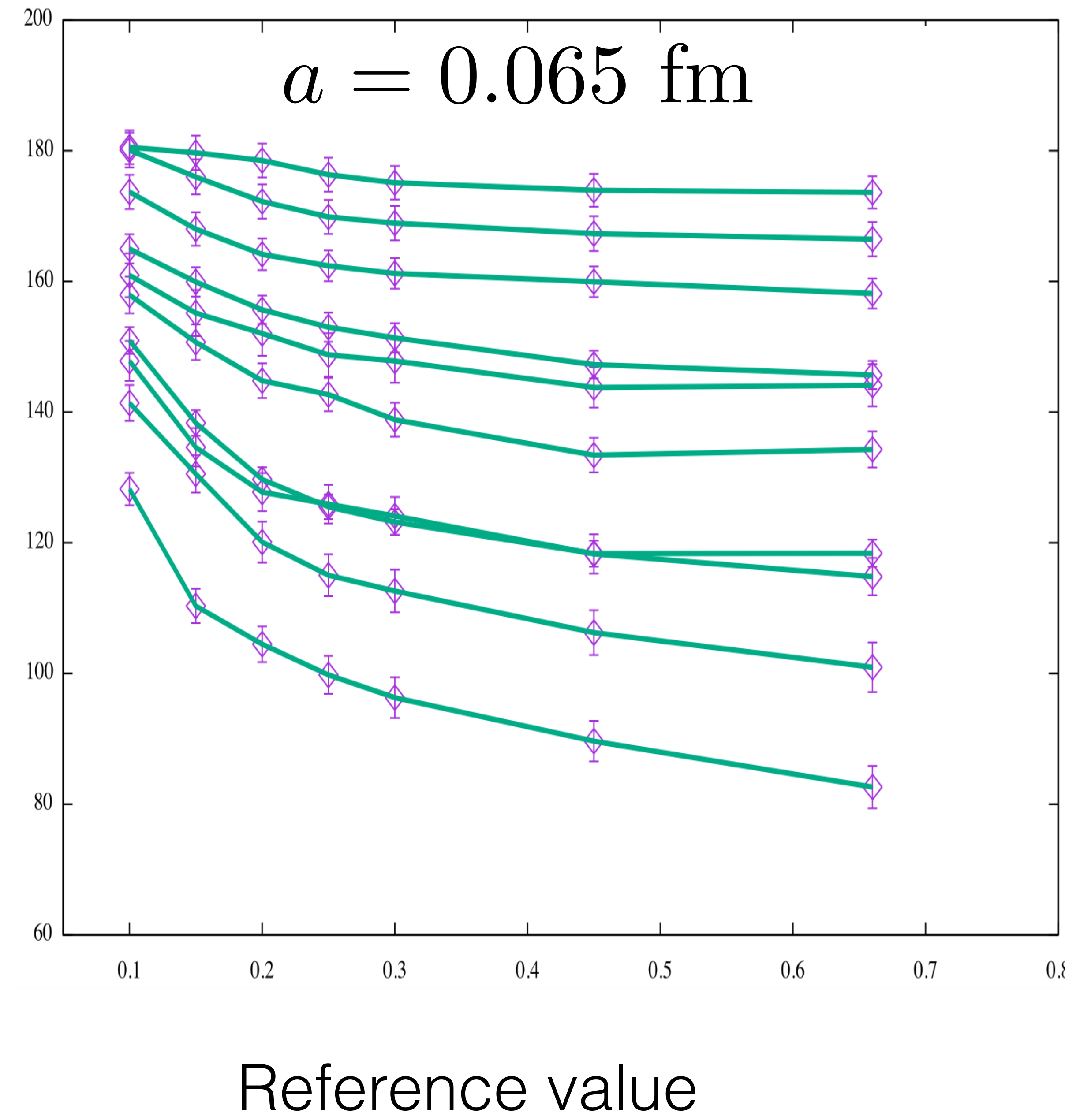

Results for the topological susceptibility for $M_\pi = 270 \text{ MeV}$

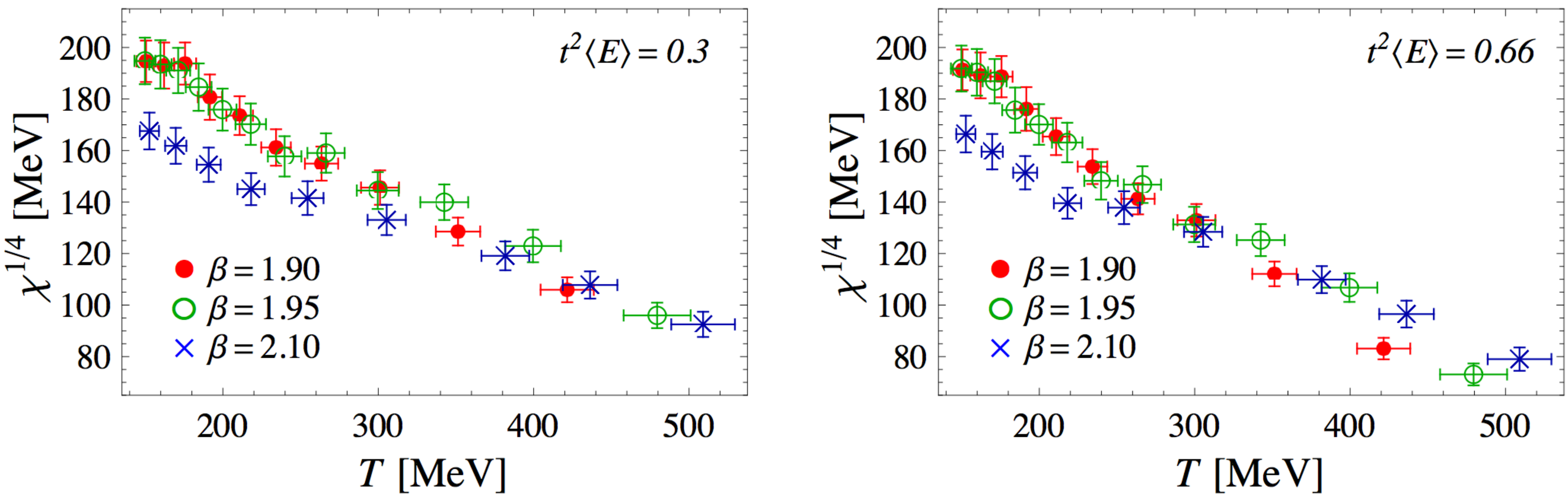

Continuum limit:

- in principle independent on flow limit
- we need to interpolate results at fixed scale to match T

$$\chi(T, m_\pi) = \lim_{a\to 0} \chi^{1/4}(T, a, m_\pi, t_x)$$

$$\chi^{1/4}(T, a, m_\pi, t_x) = \chi^{1/4}(T, m_\pi) + a^2 k(T, t_x)$$

Continuum results for $m_\pi = 370 \text{ MeV}$

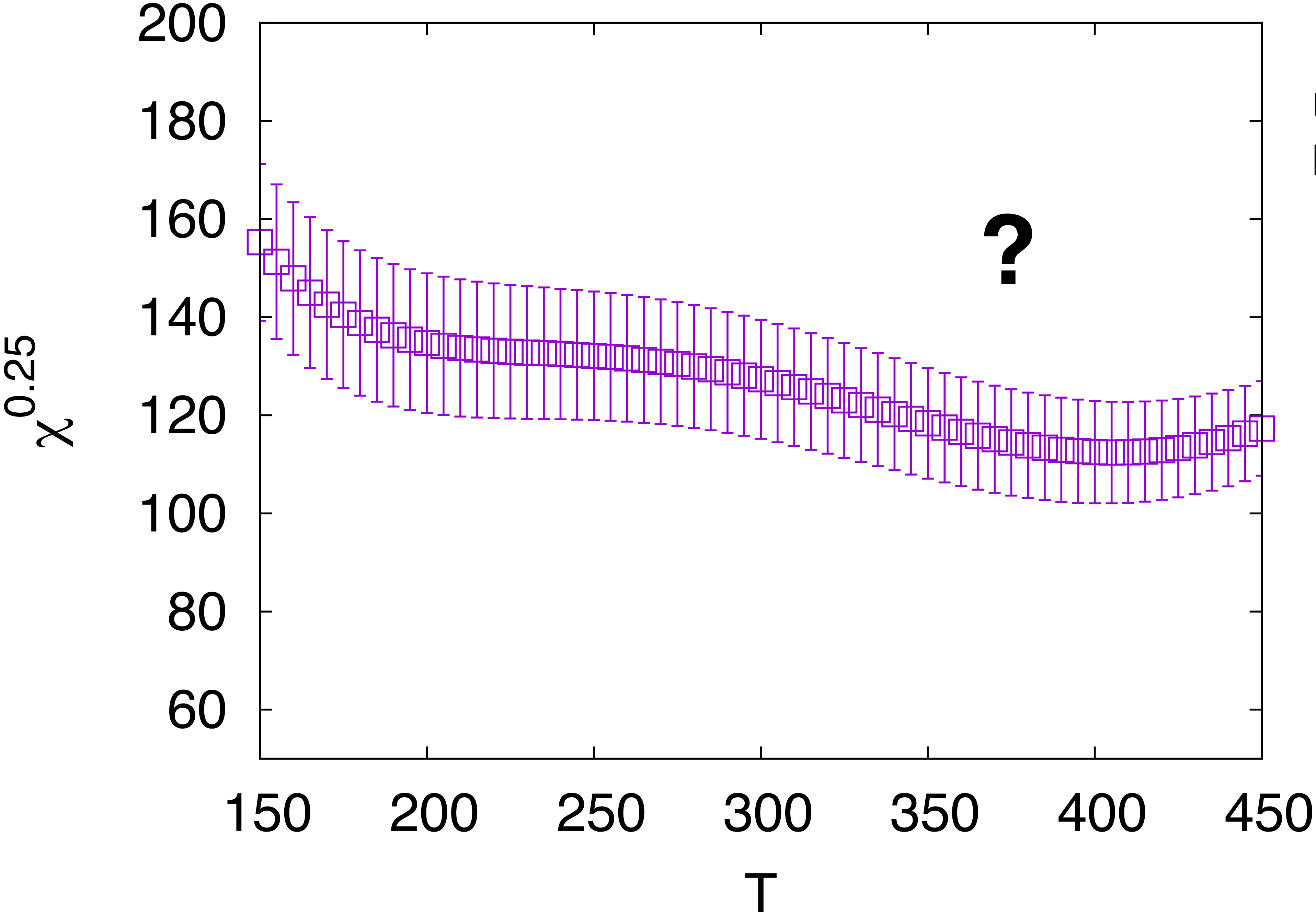

Used:
Bezier interp.

Very slow decay:
Nearly linear,
or power-like with a
tiny exponent:

$$\chi(T)^{0.25} \simeq aT^{-0.26} \simeq T, T > 200 \text{ MeV}$$

A mass rescaling appears to work nicely

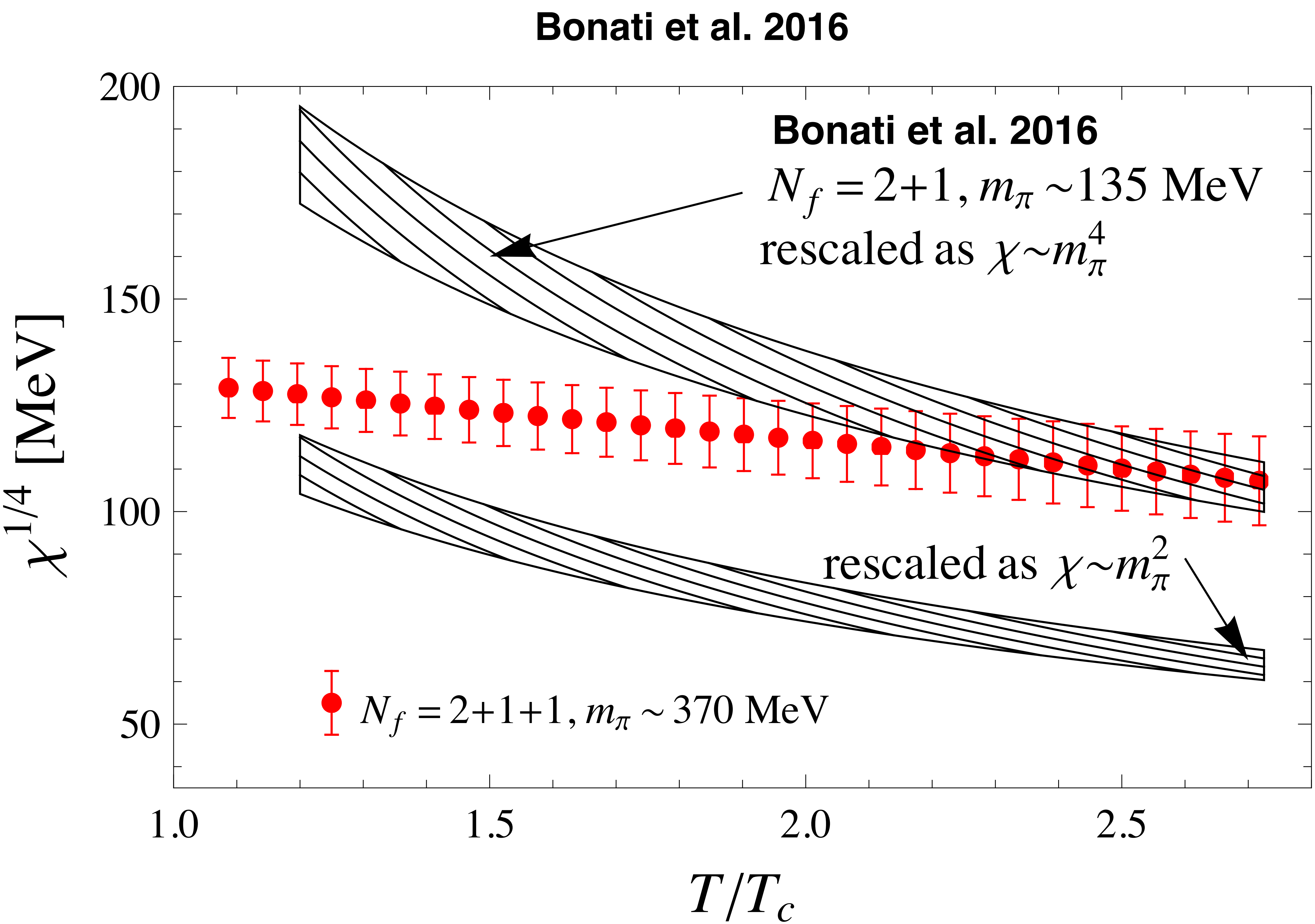

However: there is no mass dependence..

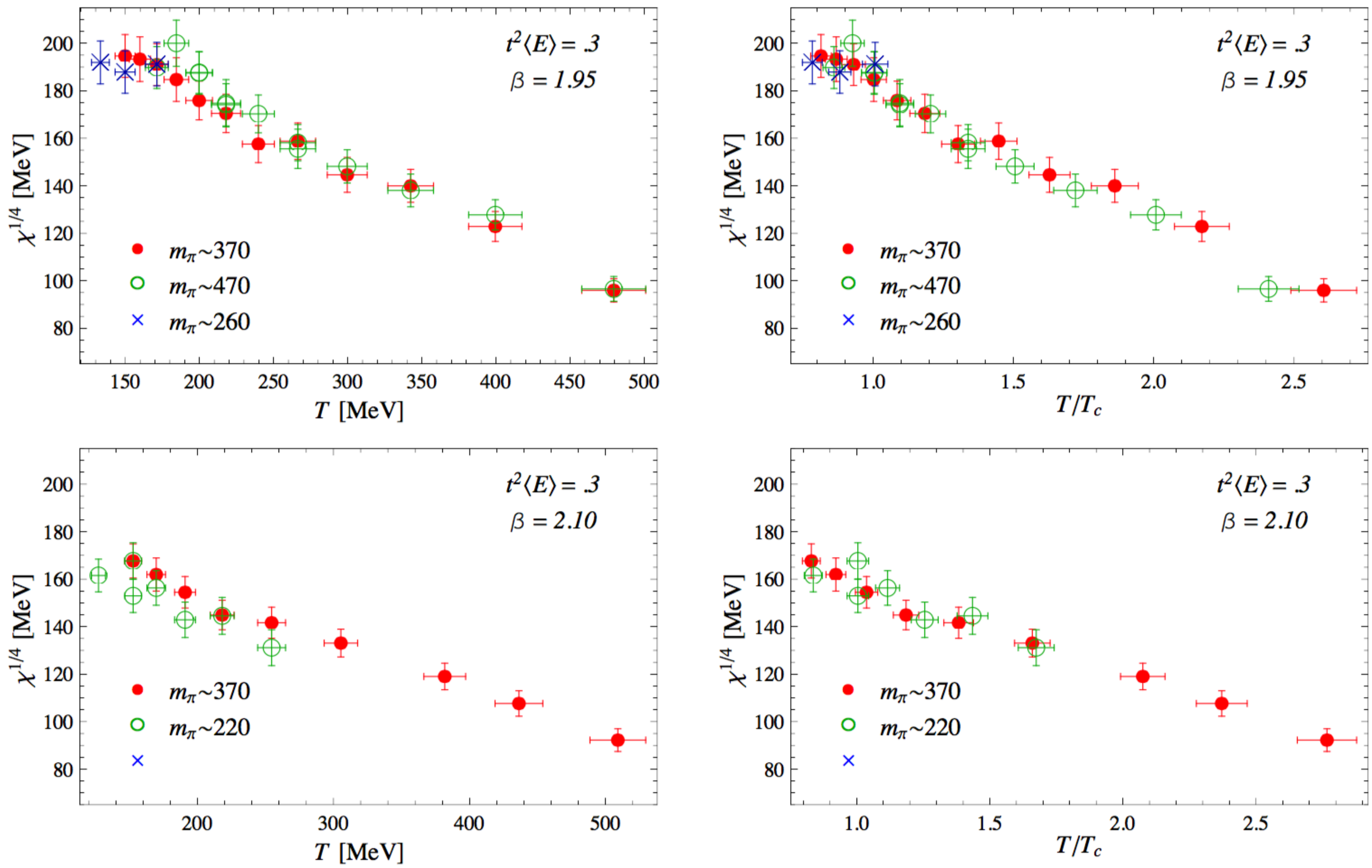

Possible explanation : strong scaling violations

Comparison with BNL results

numerical data courtesy *S. Sharma*

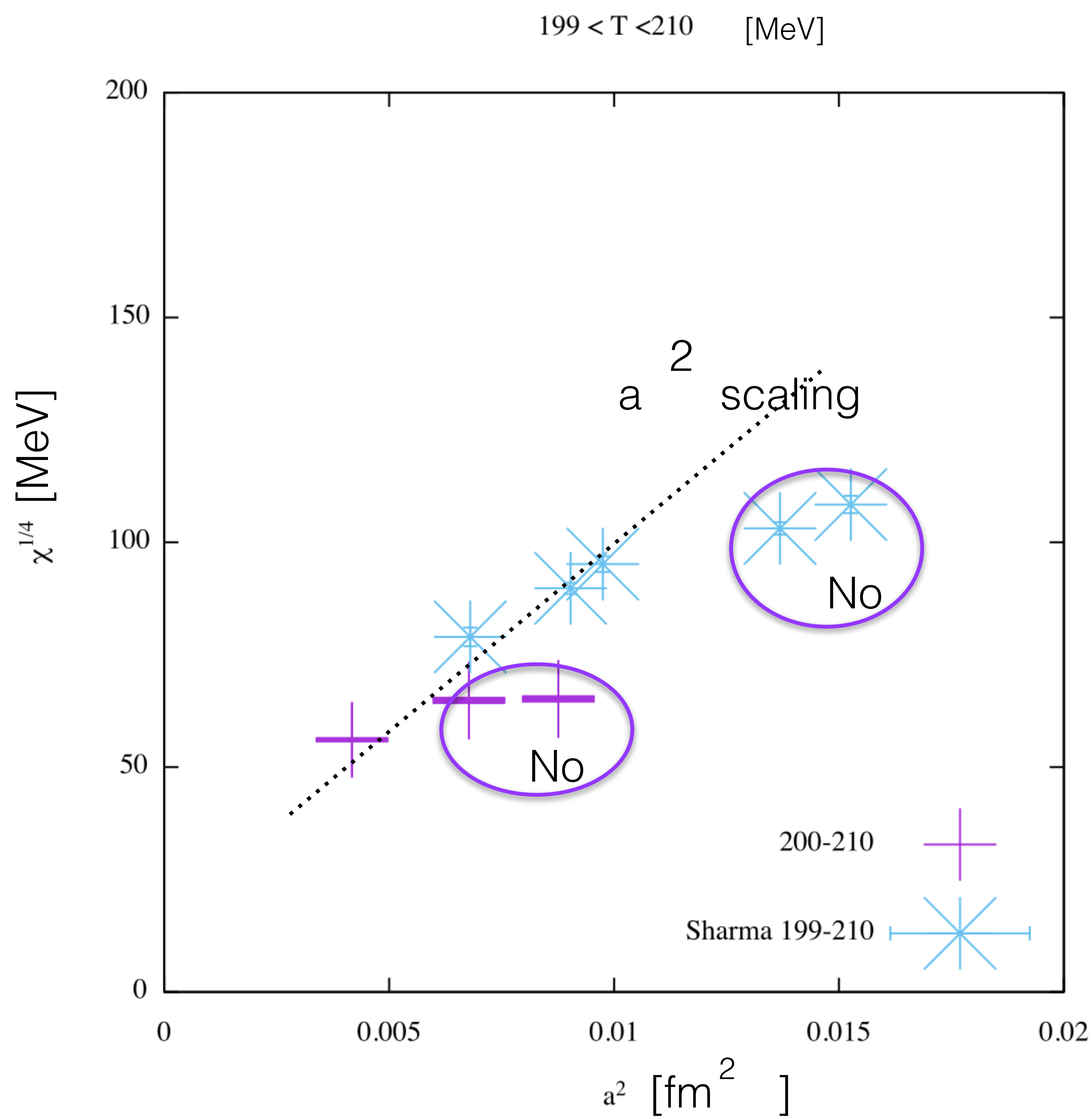

Indication of corrections to a^2 scaling on our two coarser lattices

Comparison with BNL results (contn'd)

numerical data courtesy *S. Sharma*

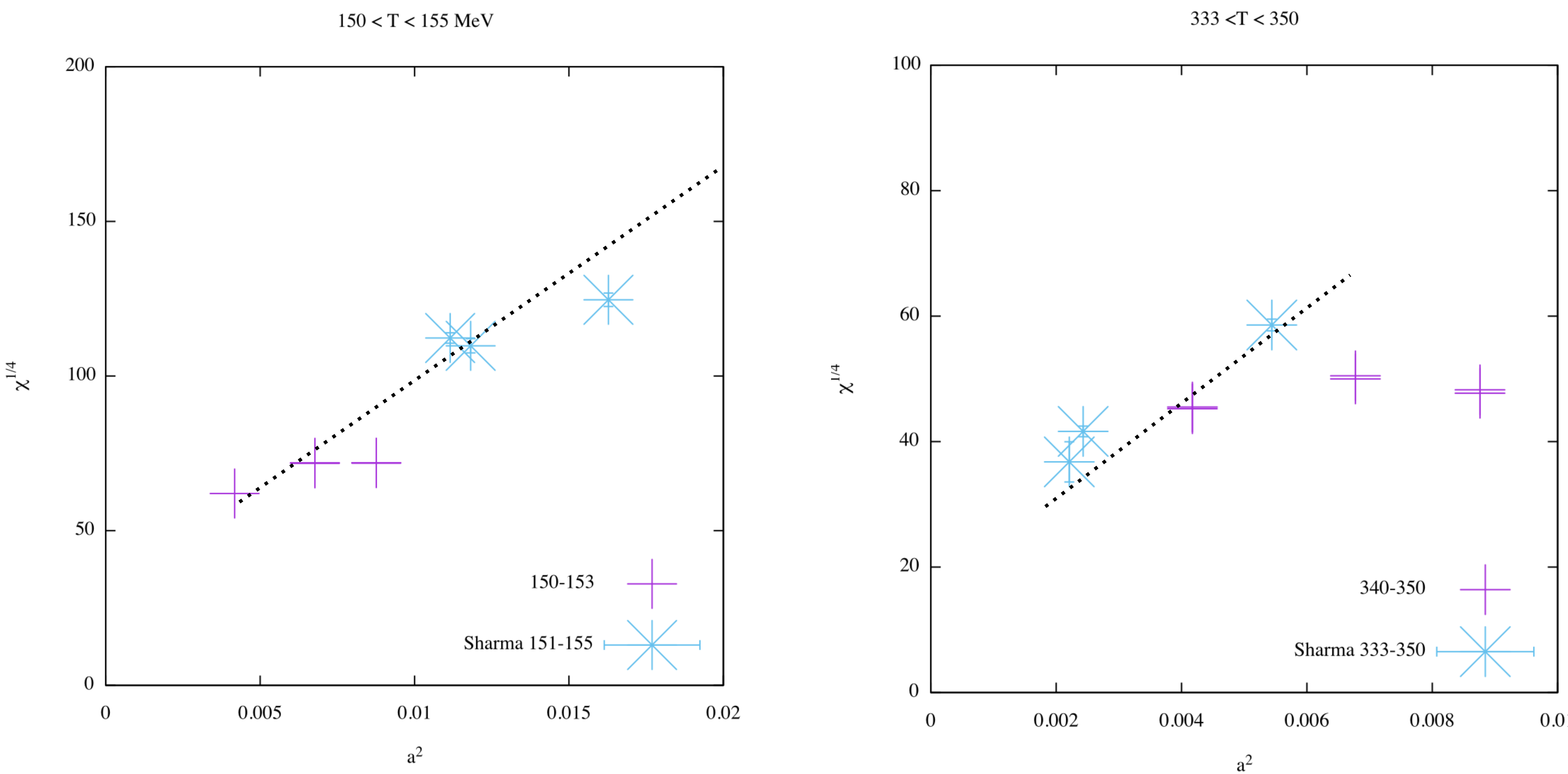

Consistent trend for other temperatures: on our finer lattice the corrections to a^2 scaling seem moderate

Instanton potential - cumulants' ratio b2

DIGA predicts

$$F(\theta,T) - F(0,T) = \chi(T)(1 - cos(\theta)) \longrightarrow b_2 = -1/12$$

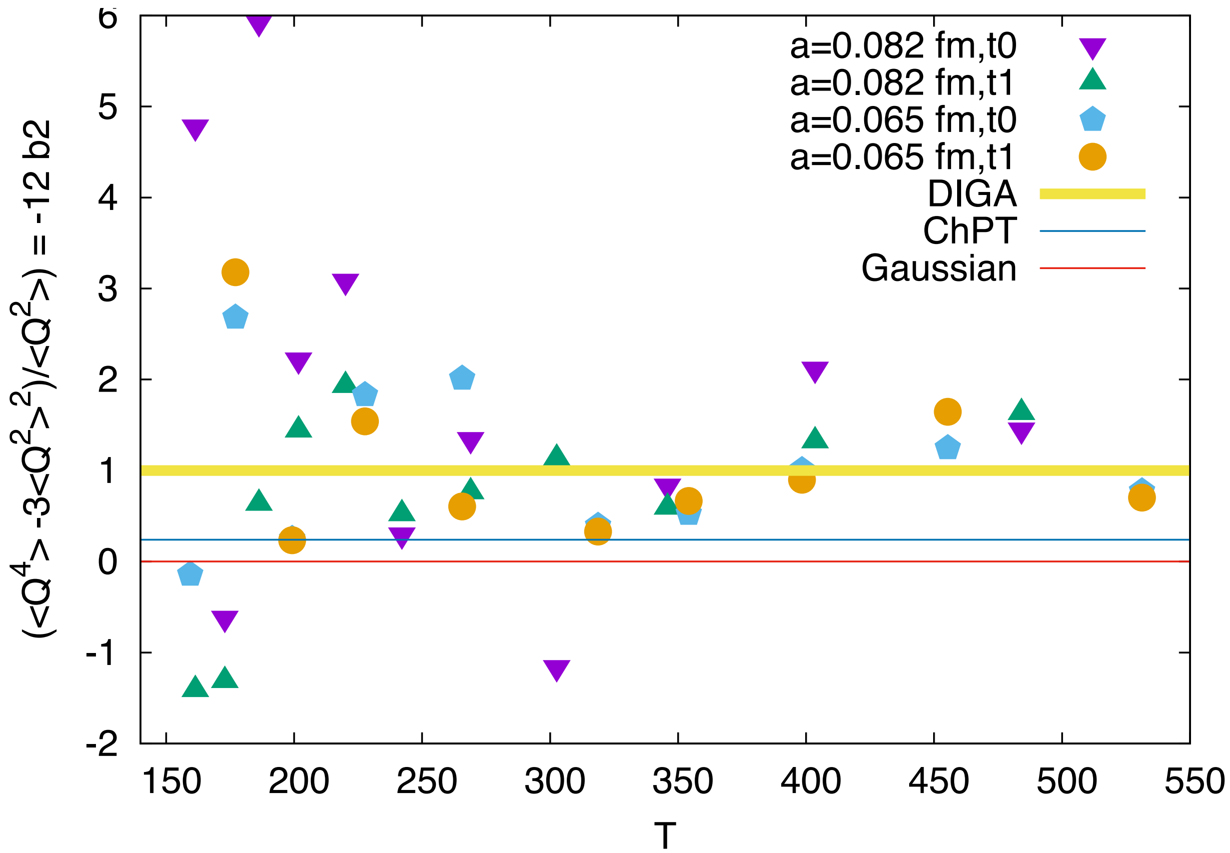

b2 = -1/12

DIGA limit for T > 350 MeV

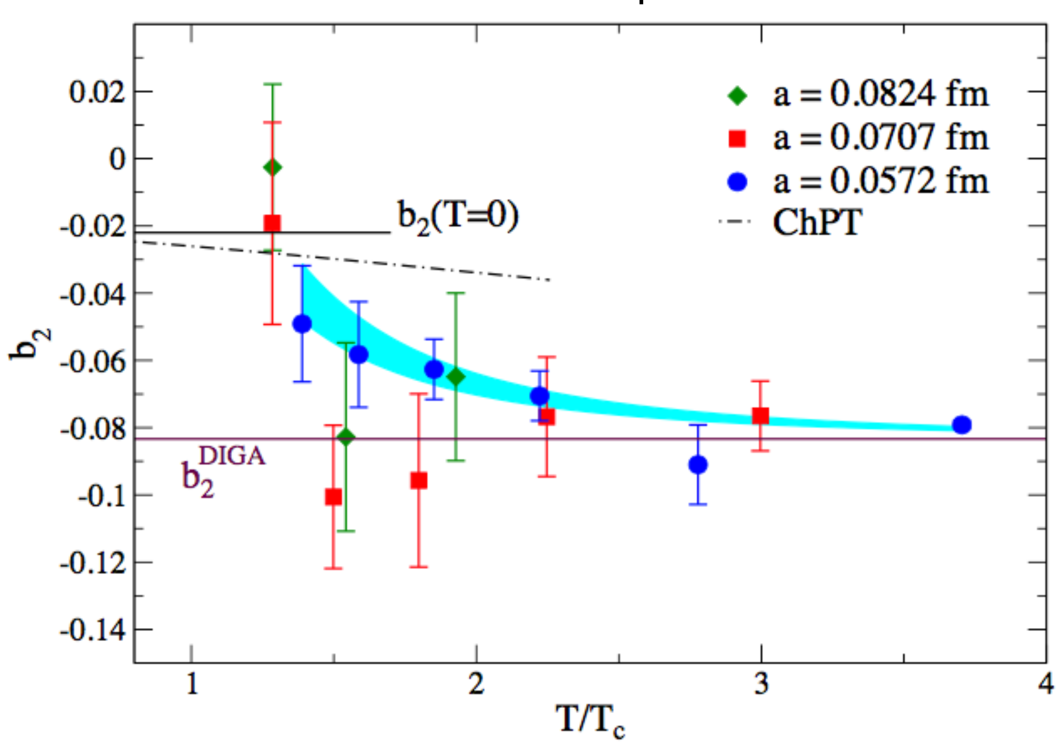

Consistent with Bonati et al.

Results II

Fermionic operator

$$n_L - n_R = Q_{top}$$

$$m \int d^4x \bar{\psi} \gamma_5 \psi = Q_{top}$$

Topological and chiral susceptibility

Kogut, Lagae, Sinclair 1999

HotQCD, 2012

$$\chi_{top} =< Q_{top}^2 > /V = m_l^2 \chi_{5,disc}$$

From:

$$m \int d^4x \bar{\psi}\gamma_5\psi = Q_{top}$$

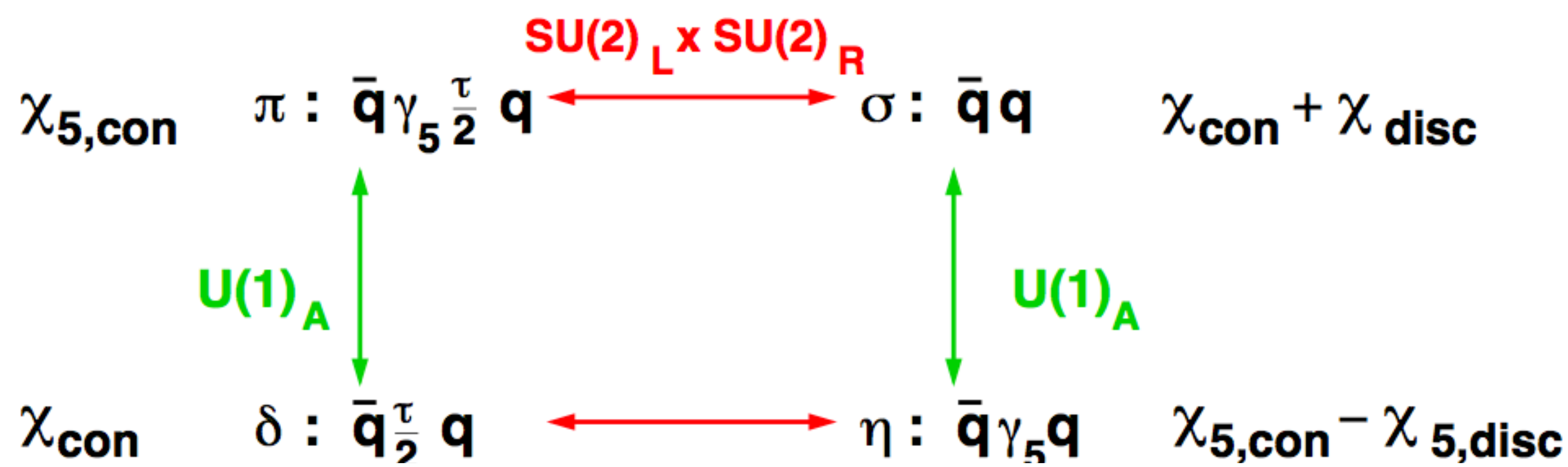

$$\chi_\pi - \chi_\delta = \chi_{\rm disc} = \chi_{\rm 5,disc} \; , \qquad \text{for} \quad T \geq T_c \; , \; m_l \to 0$$

$$\chi_{top} =< Q_{top}^2 > /V = m_l^2 \chi_{disc}$$

$$T > T_{U(1)_A} \simeq T_c$$

Chiral susceptibility

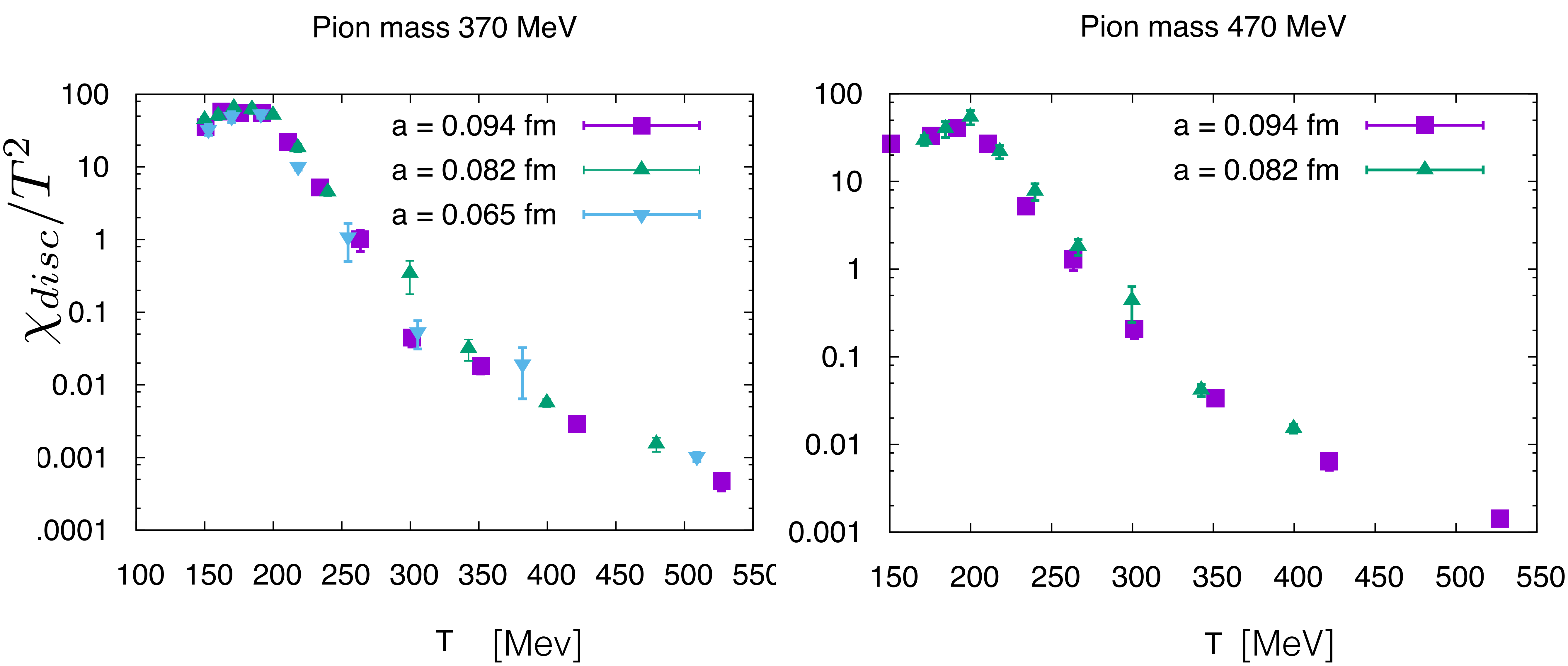

Within errors, no discernable spacing dependence

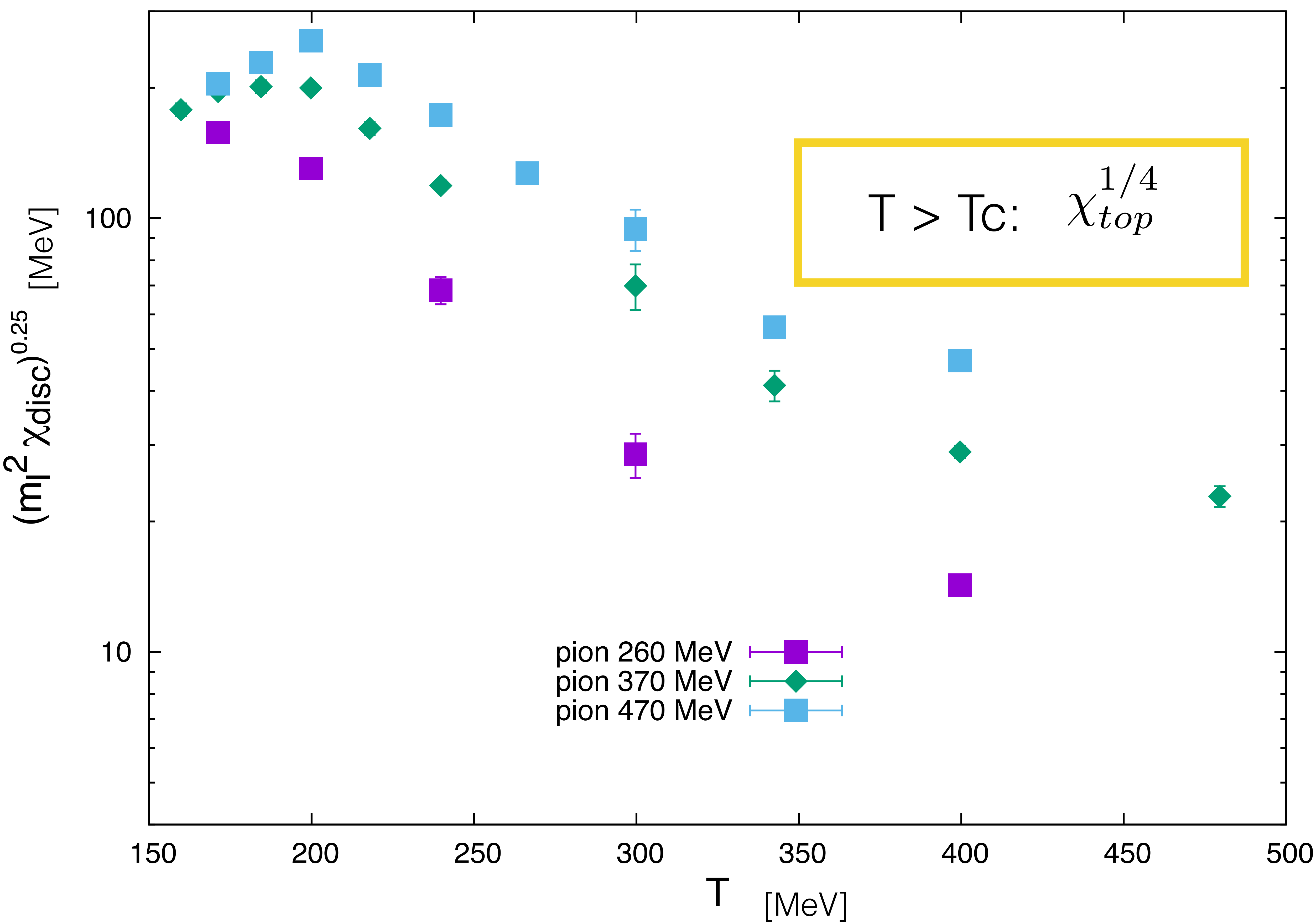

T > Tc: $\chi_{top}^{1/4}$
$(m_l^2\chi disc)^{0.25}$ [MeV]
100
10
150
200
250
300
350
400
450
500
T [MeV]
pion 260 MeV
pion 370 MeV
pion 470 MeV

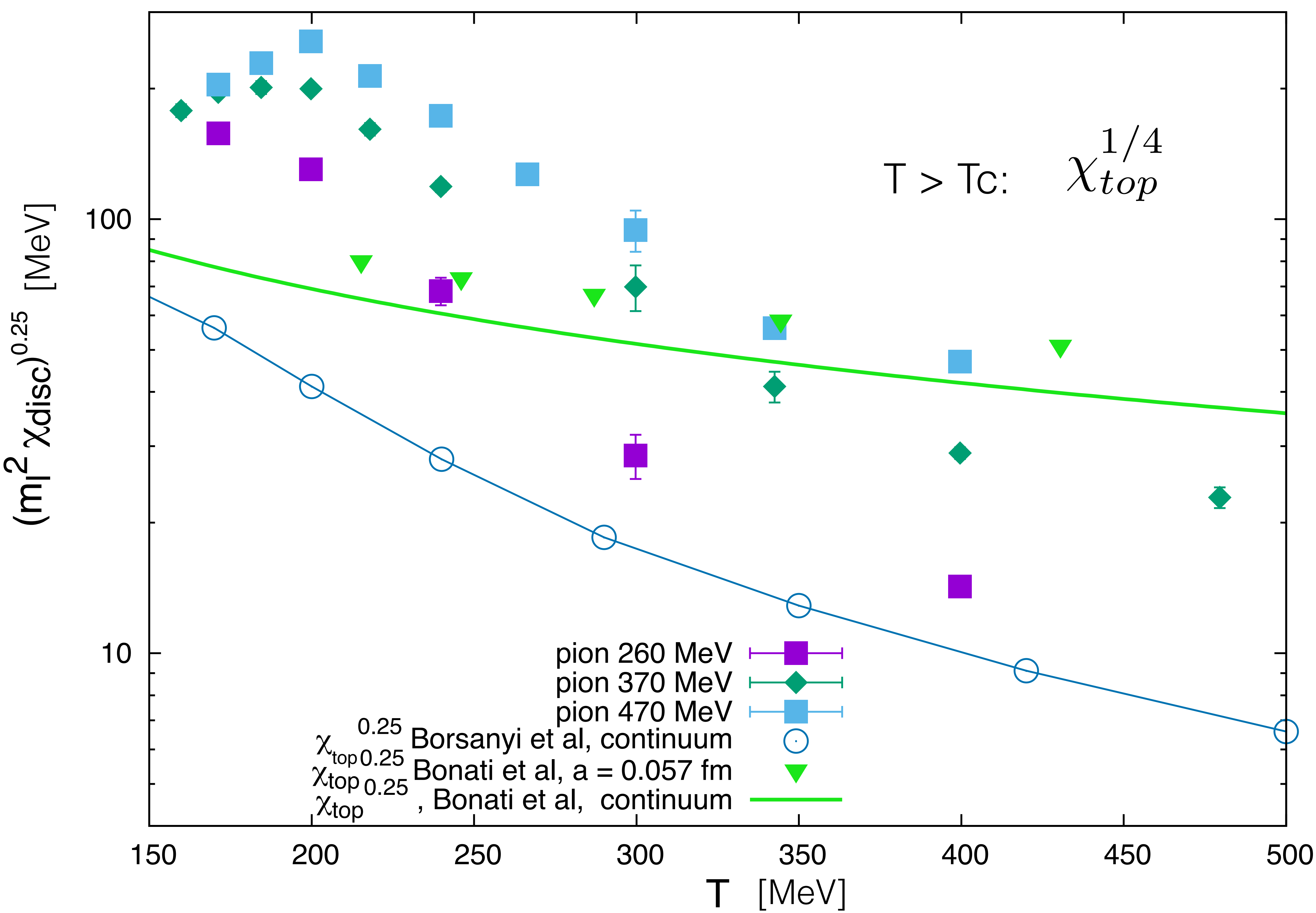

T > Tc: $\chi_{top}^{1/4}$
$(m_l^2 \chi disc)^{0.25}$ [MeV]
100
10
150
200
250
300
350
400
450
500
T [MeV]
pion 260 MeV
pion 370 MeV
pion 470 MeV
$\chi_{top}^{0.25}$ Borsanyi et al, continuum
$\chi_{top}^{0.25}$ Bonati et al, a = 0.057 fm
$\chi_{top}^{0.25}$, Bonati et al, continuum

Results for physical pion mass

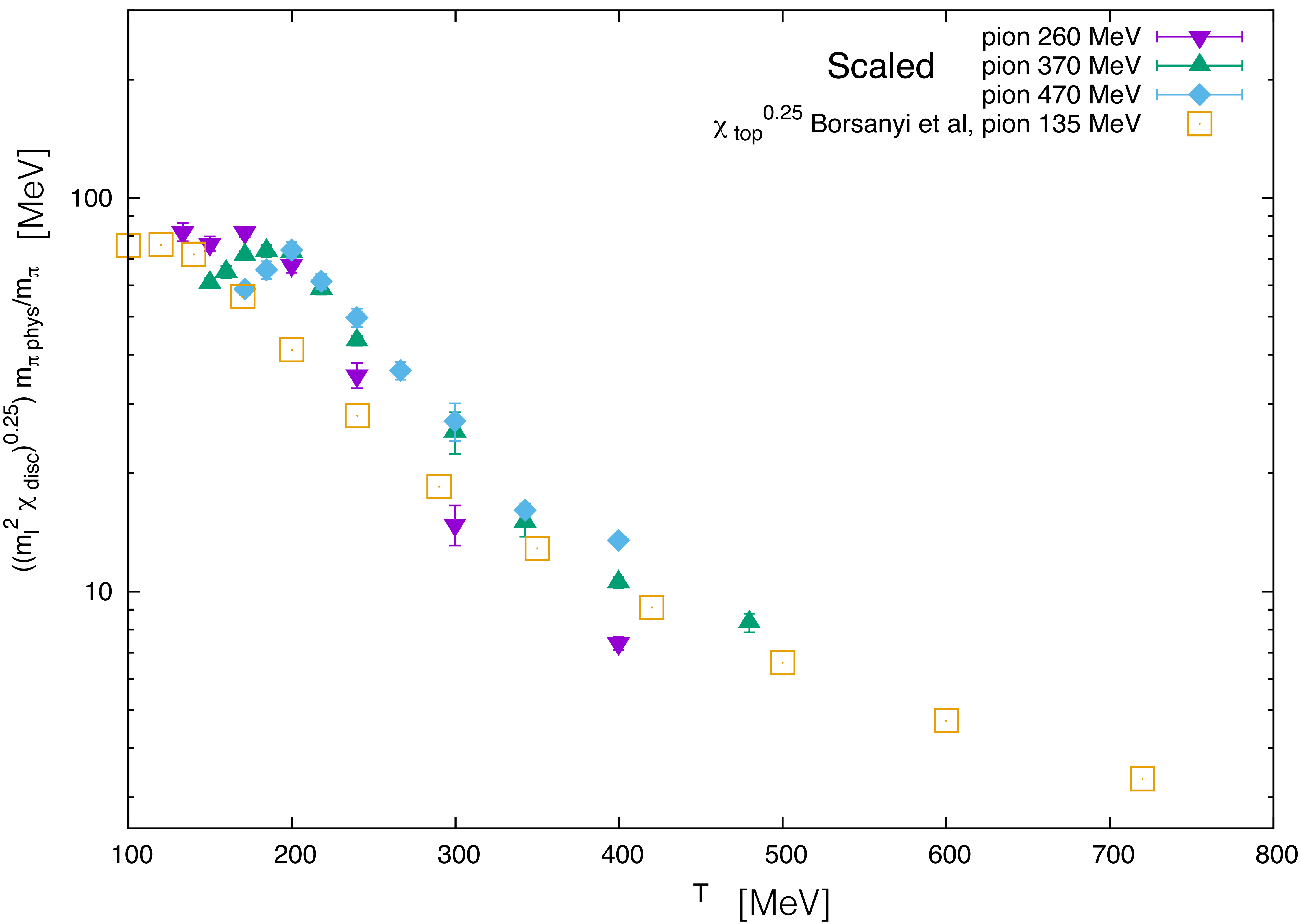

Comparison with BNL results including fermionic results

numerical data courtesy *S. Sharma*

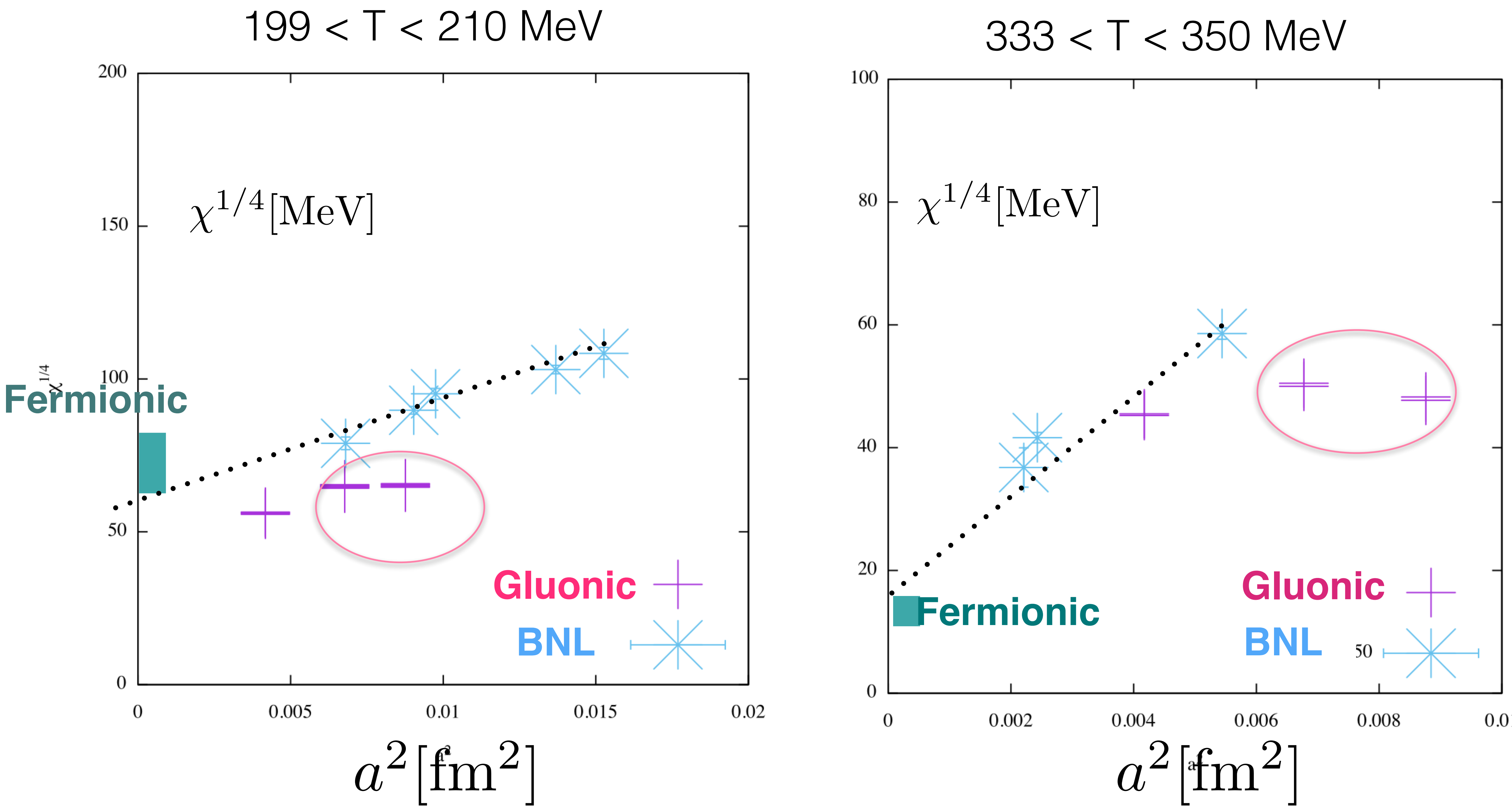

dotted lines to guide the eye

Effective exponent : $$d(T) = -T\frac{d}{dT}\ln\chi^{0.25}(T)$$

$$\chi^{0.25}(T) = aT^{-d(T)}$$

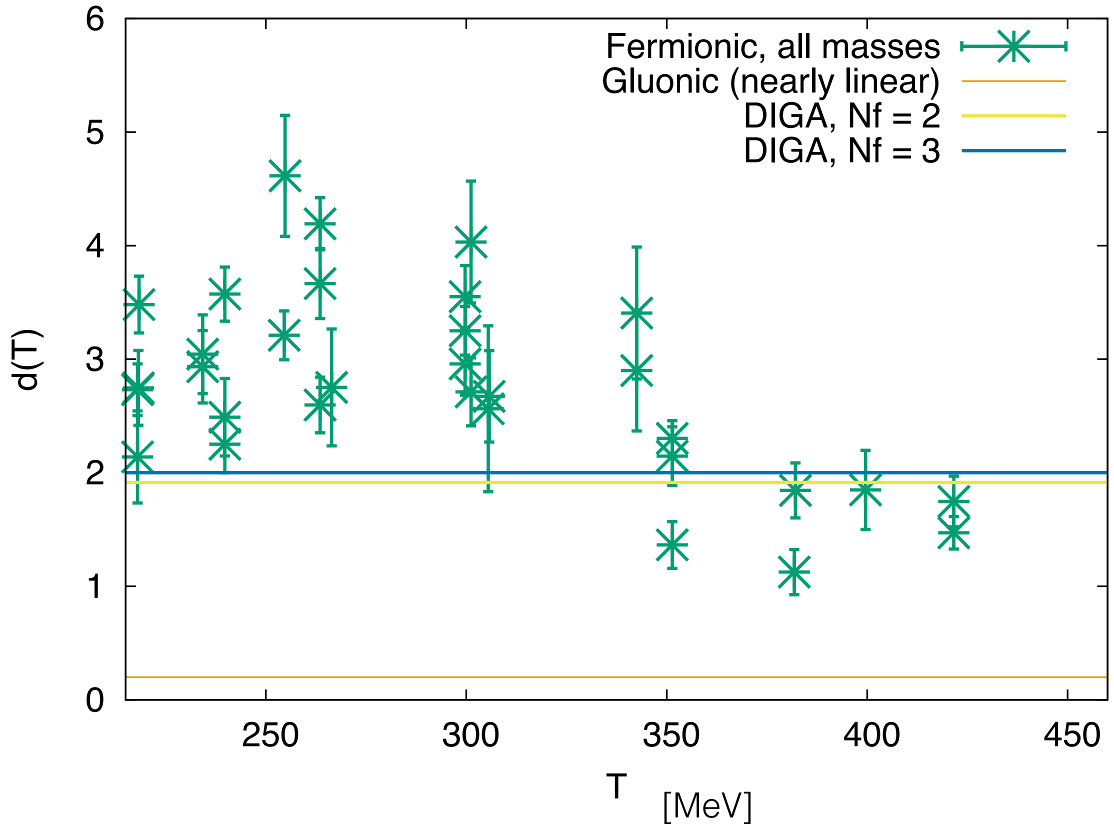

Possibly consistent with instant -dyon? Shuryak 2017

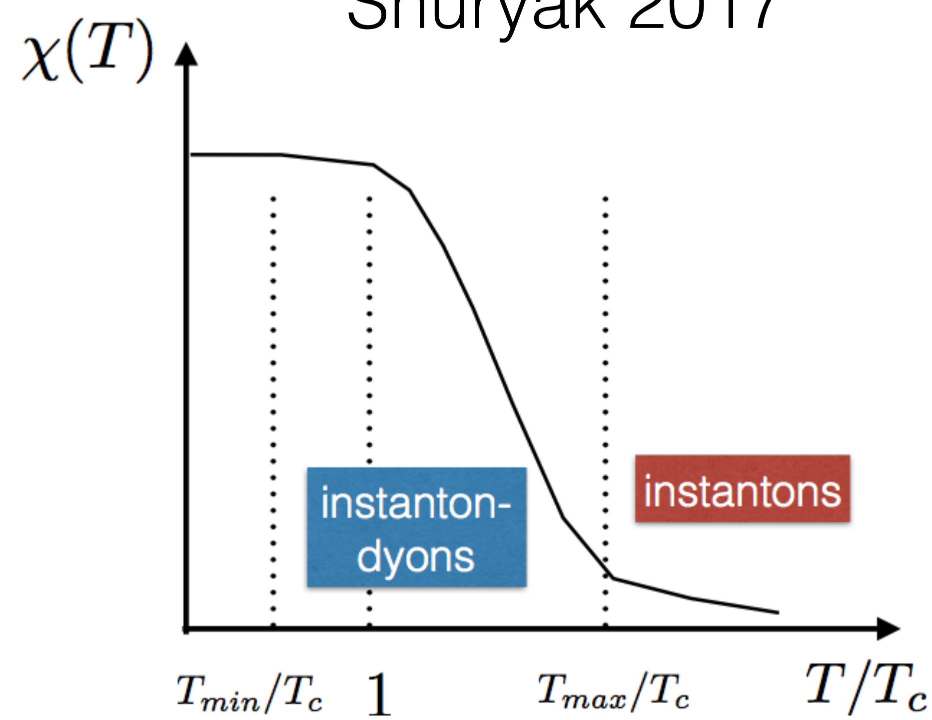

Faster decrease before DIGA sets in

Effective exponent :

$$\chi_{top}^{1/4} = aT^{-d(T)}$$

Same DIGA onset seen in b2 ≈ 350 MeV

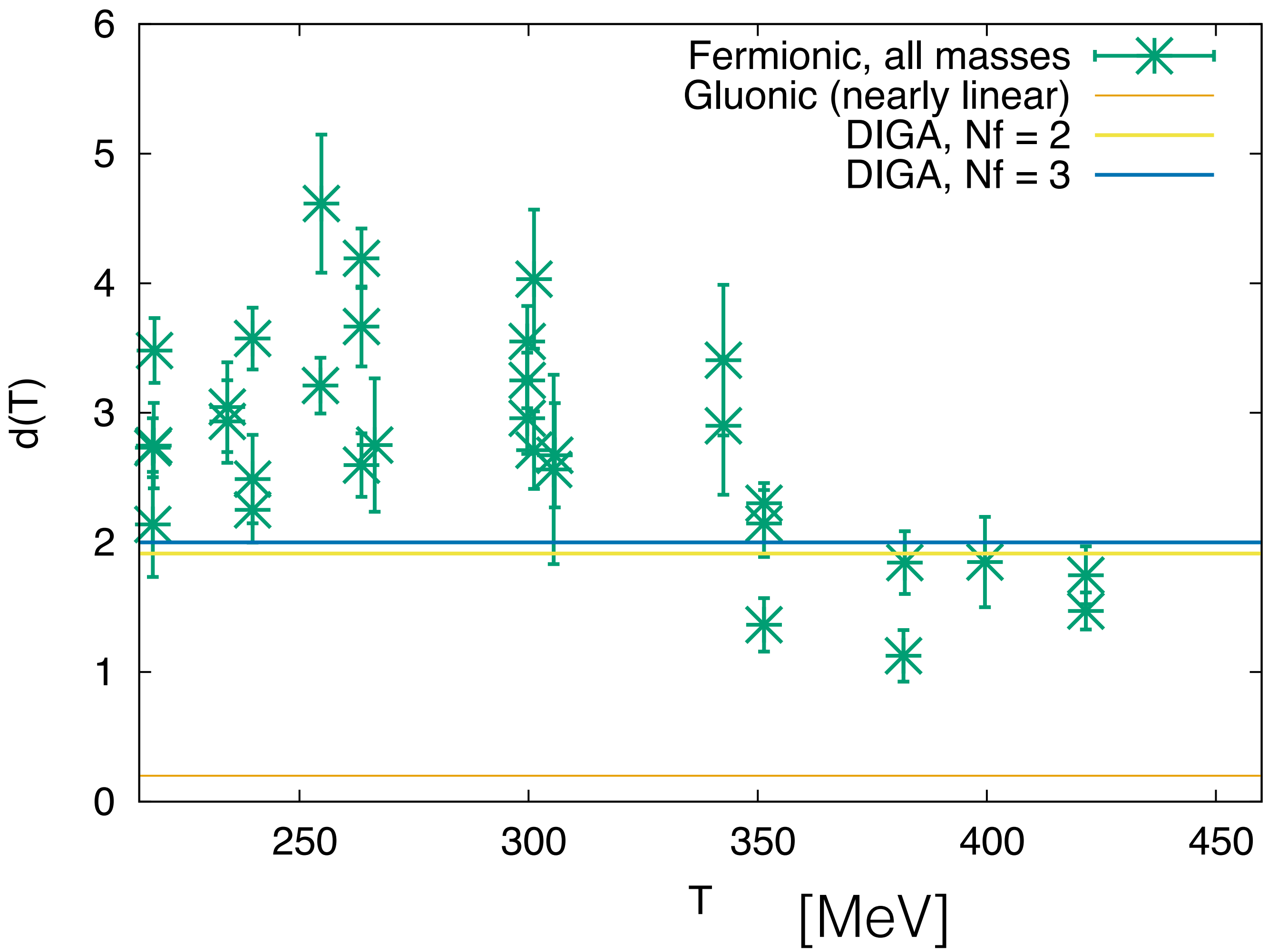

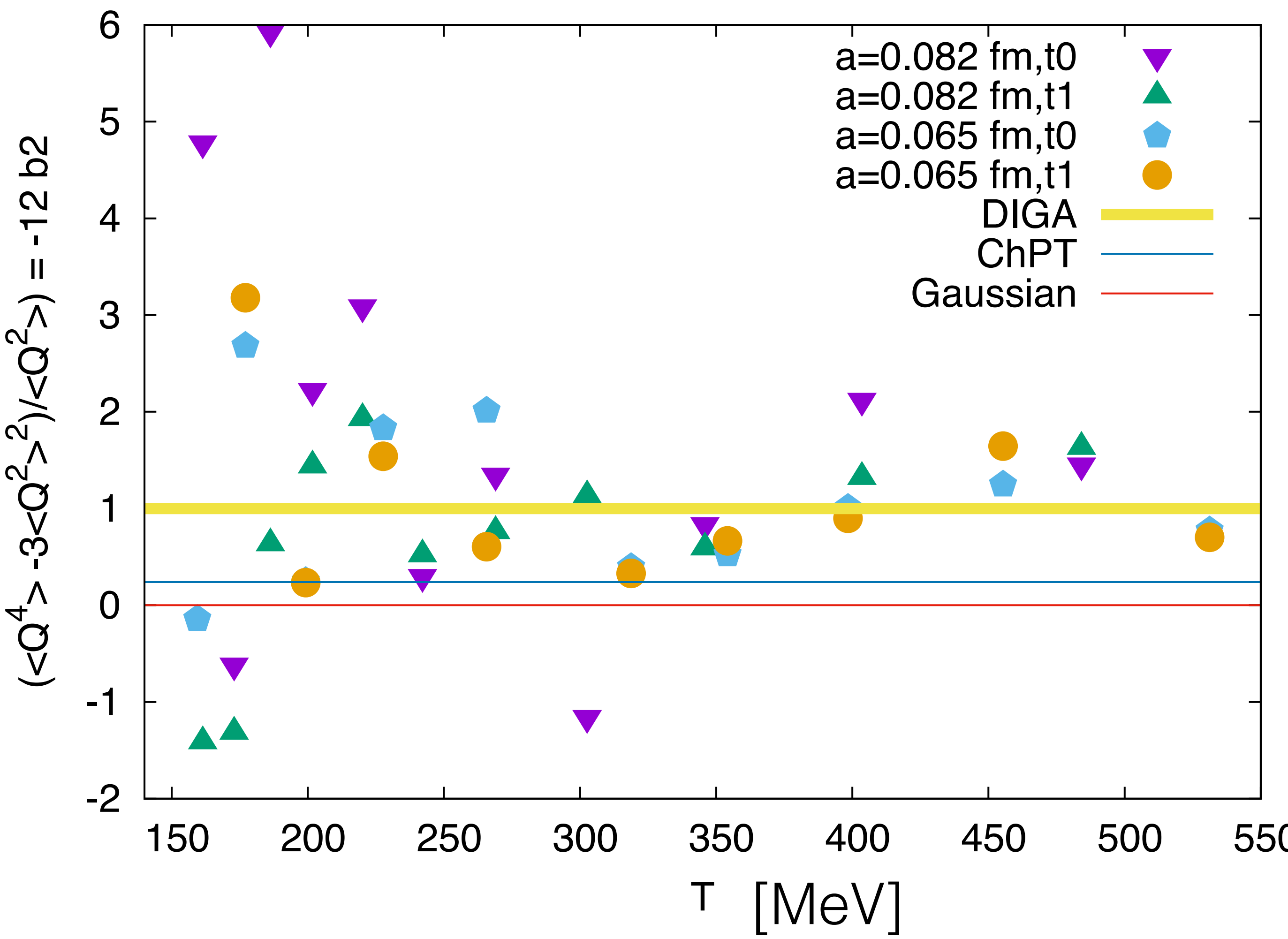

Effective exponent d(T):

Comparisons with other results :

$$\chi_{top}^{1/4} = aT^{-d(T)}$$

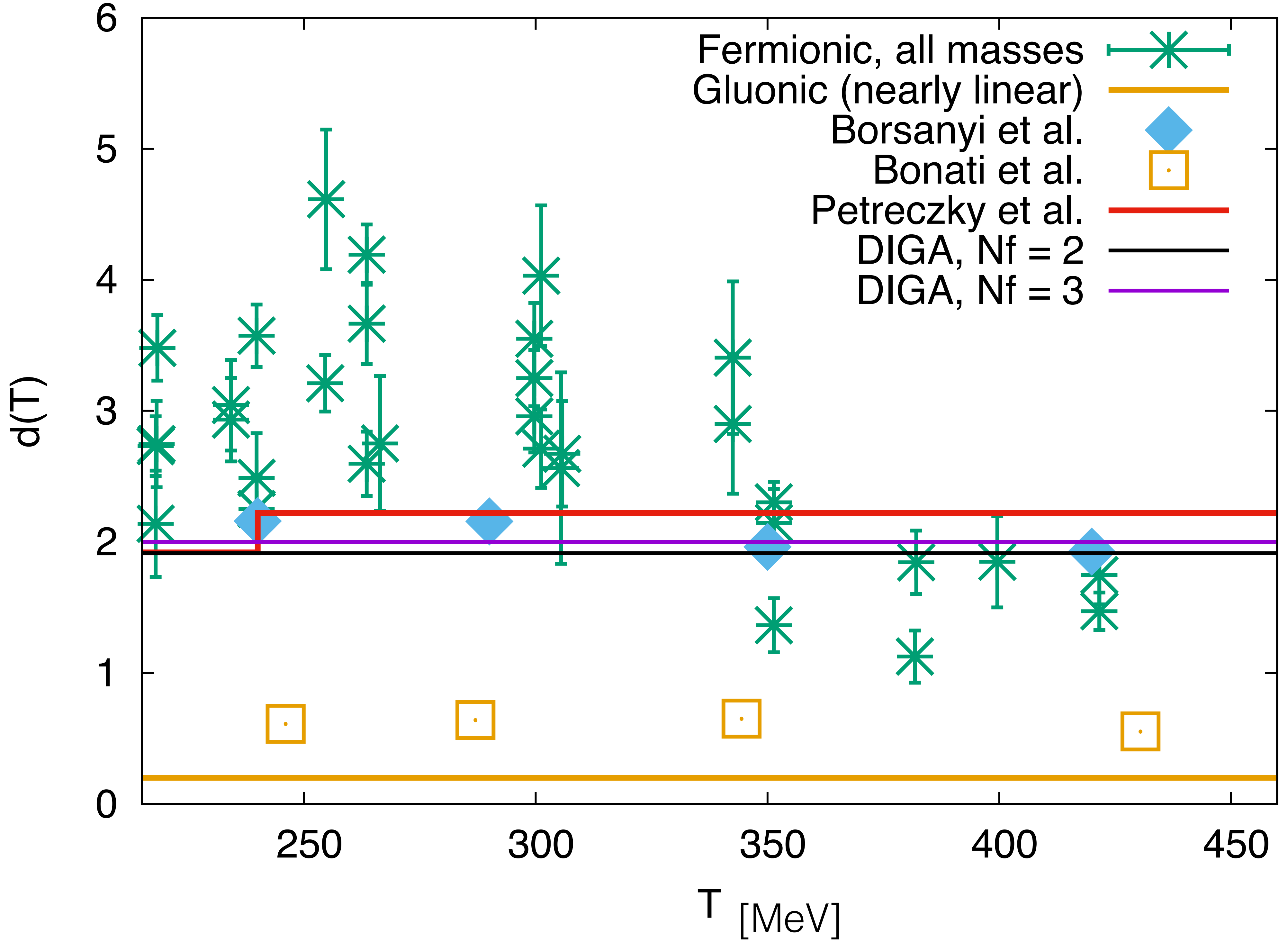

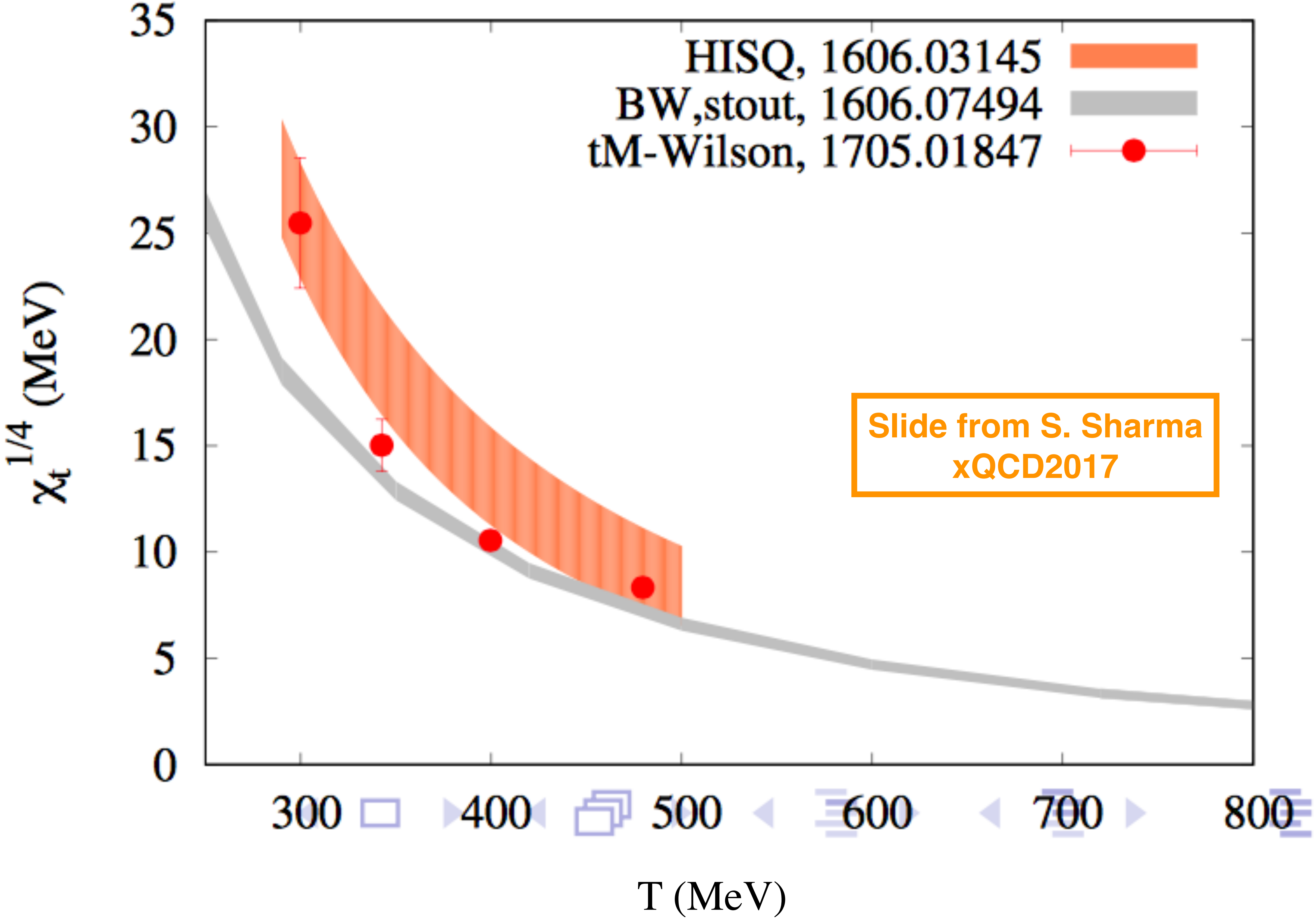

HISQ, 1606.03145
BW,stout, 1606.07494
tM-Wilson, 1705.01847
Slide from S. Sharma
xQCD2017
$\chi_t^{1/4}$ (MeV)
T (MeV)
0
5
10
15
20
25
30
35
300
400
500
600
700
800

A window on the axions

Inspiring paper:
Berkowitz, Buchoff, Rinaldi **Phys.Rev. D92 (2015) no.3, 034507**

Theory landscape (From Tim Tait, Snowmass)

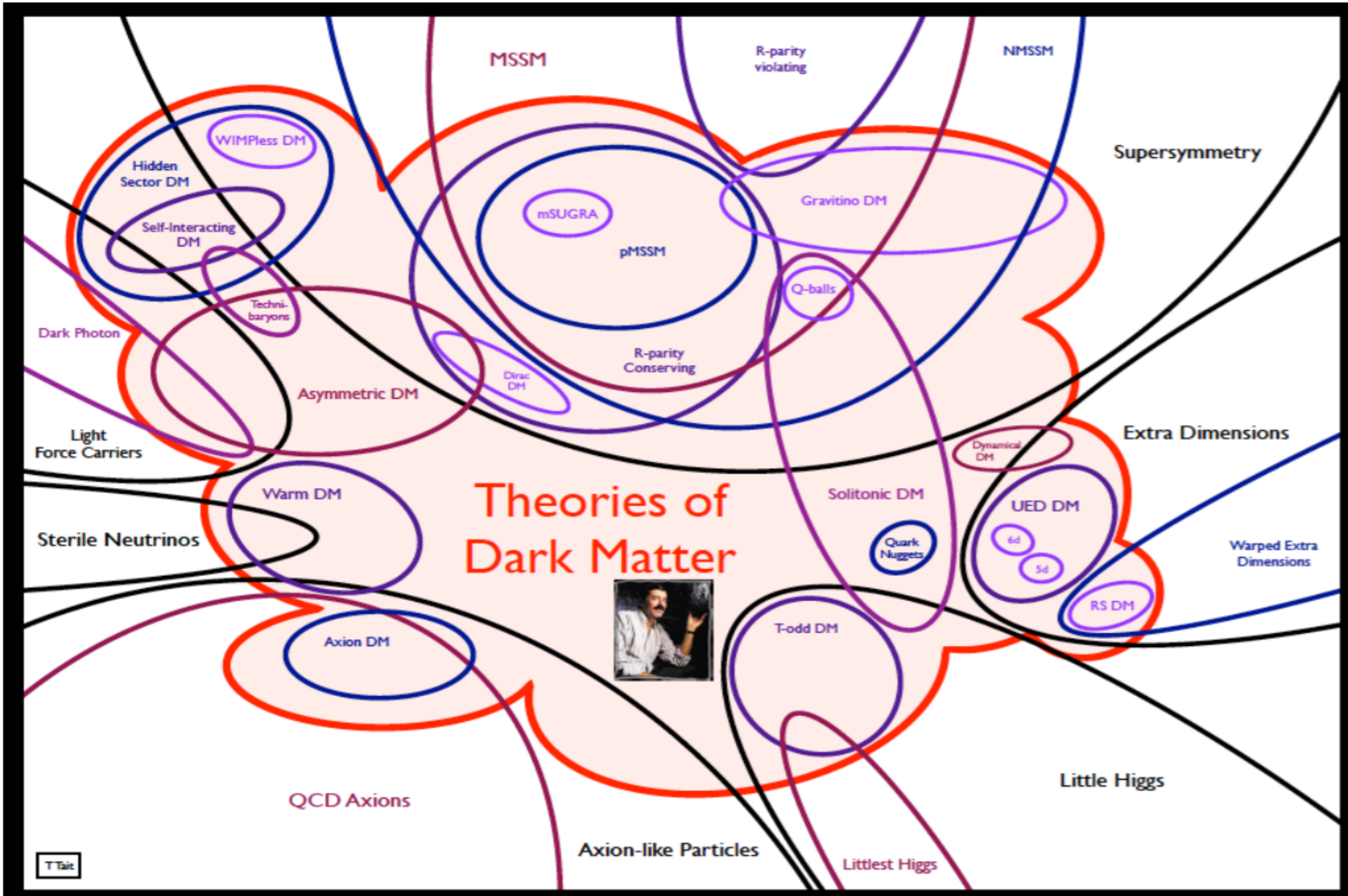

The Equation of State of the Quark Gluon Plasma paves the way to Cosmology

Cold Dark Matter candidates might have been created after the inflation

Several CDM candidates are highly speculative - but one, **the axion**, is

Theoretically well motivated in QCD
Amenable to quantitative estimates once QCD topological properties are known:

$$m_a(T) = \sqrt{\chi(T)}/f_a$$

Post-inflationary axions

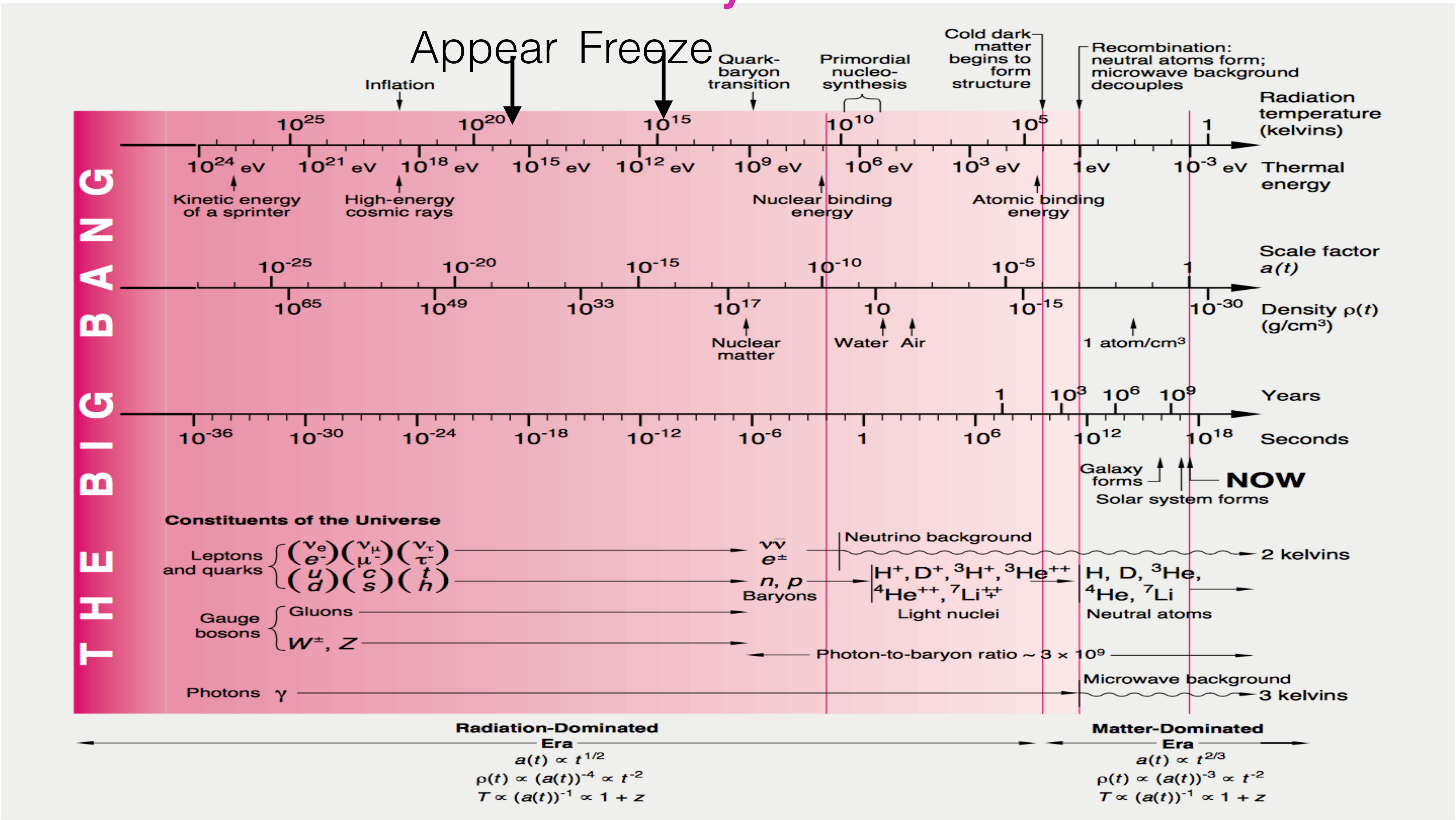

Axions ‘must’ be there: solution to the strong CP problem

$$\mathcal{L}_{QCD}(\theta) = \mathcal{L}_{QCD} + \frac{g^2\theta}{32\pi^2}\epsilon^{\mu\nu\rho\sigma}F^a_{\mu\nu}F^a_{\rho\sigma}.$$

Ammitted but $\theta < 10^{-9}$

$$Q = \int d^4x \, \frac{g^2}{32\pi^2}\mathrm{tr}F\tilde{F}$$

Postulate axions, coupled to Q:

$$\mathcal{L}_{\mathrm{axions}} = \frac{1}{2}\left(\partial_\mu a\right)^2 + \left(\frac{a}{f_a} + \theta\right)\frac{1}{32\pi^2}\epsilon^{\mu\nu\rho\sigma}F_{\mu\nu}F_{\rho\sigma}$$

$$Z_{QCD}(\theta, T) = \int [dA][d\psi][d\bar{\psi}] \exp\left(-T\sum_t d^3x \, \mathcal{L}_{QCD}(\theta)\right) = \exp[-VF(\theta, T)]$$

Axion potential

$$m_a^2(T) f_a^2 = \left.\frac{\partial^2 F(\theta, T)}{\partial\theta^2}\right|_{\theta=0} \equiv \chi(T),$$

Time from Big Bang

Temperatures

150 MeV < T < 500 MeV

..and beyond

Temperature and Time from BigBang are linked by the Equation of State

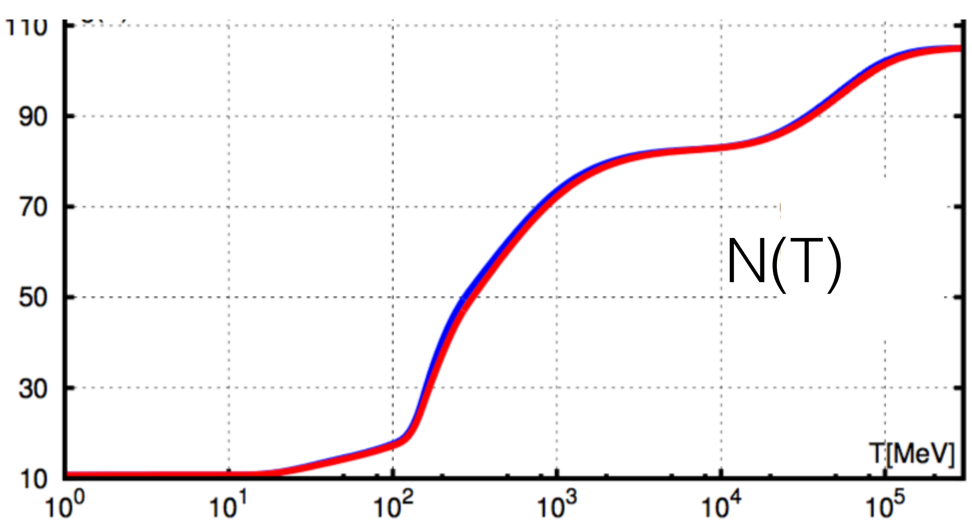

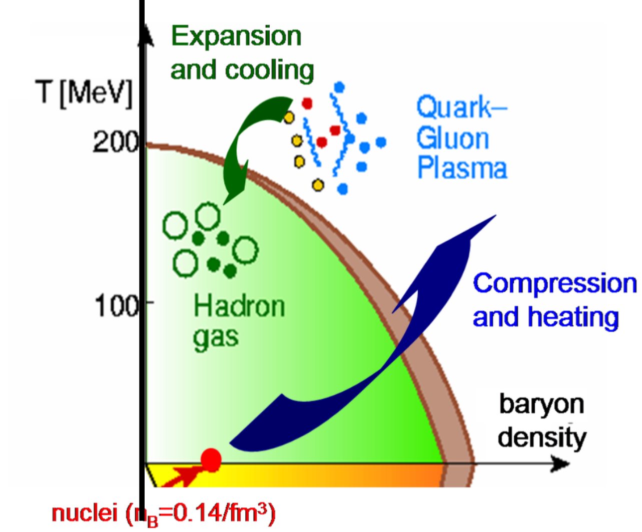

Temperature

Time from Big Bang

Hubble parameter
$$H(T) \simeq T^2/M_P$$

Axions's freezout

$$3H(T) = m_a(T)$$

$$m_a(T) = \sqrt{\chi(T)}/f_a$$

Quark Gluon Plasma:
Topology

Axions' mass
and density
today

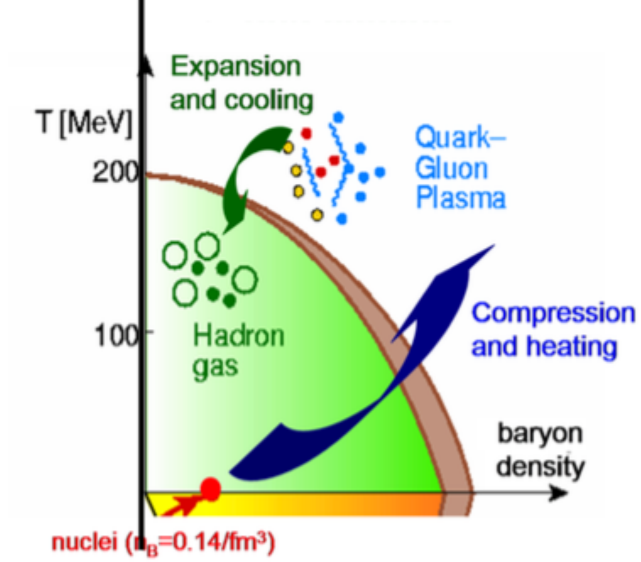

Axion freezout : $3H(T) = m_a(T) = \sqrt{\chi(T)}/f_a$

Berkowitz Buchoff Rinaldi 2015

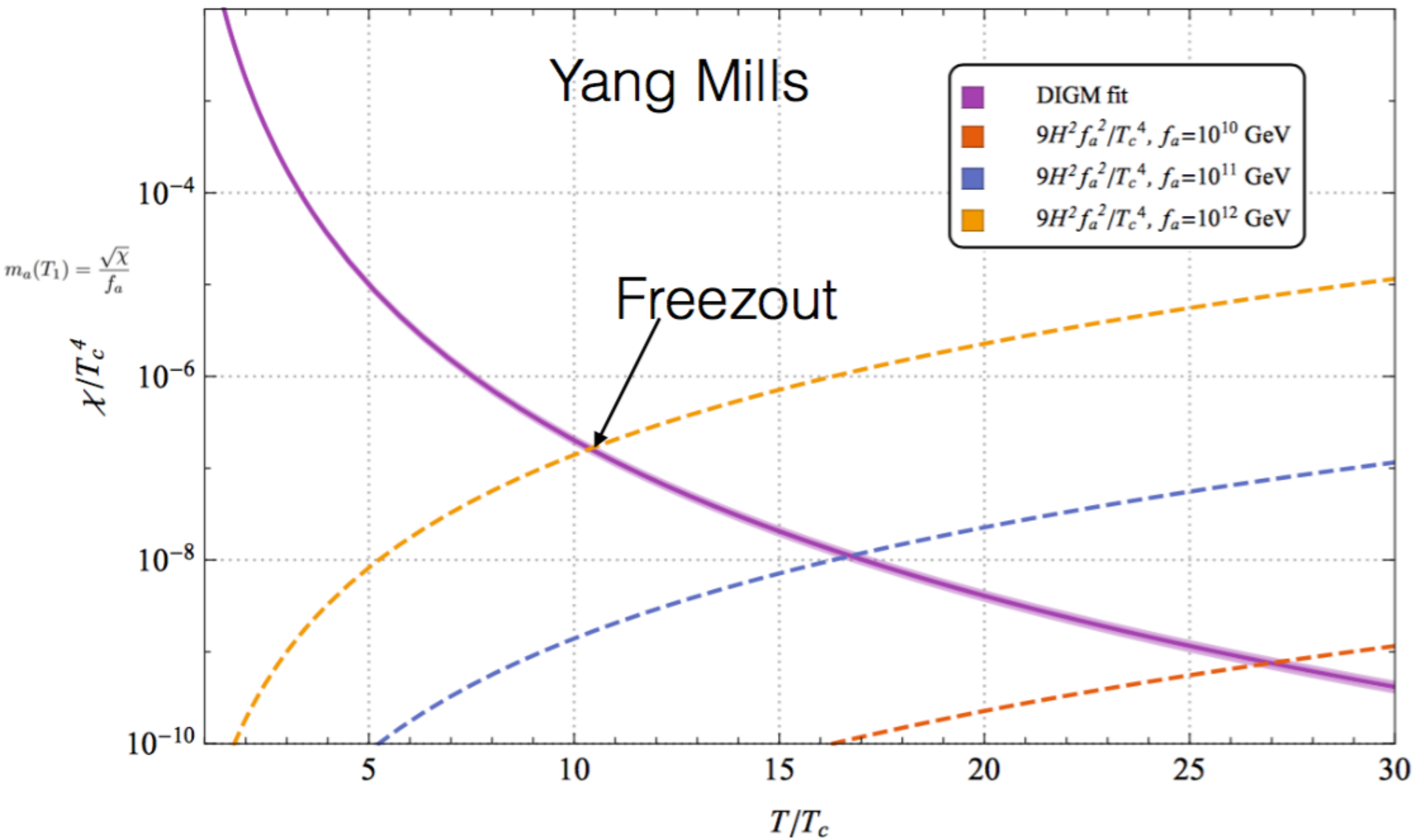

Axion density at freezout controls axion density today

Needed assumption on
fraction of DM made of axions

Assume: Axions make all of Dark Matter

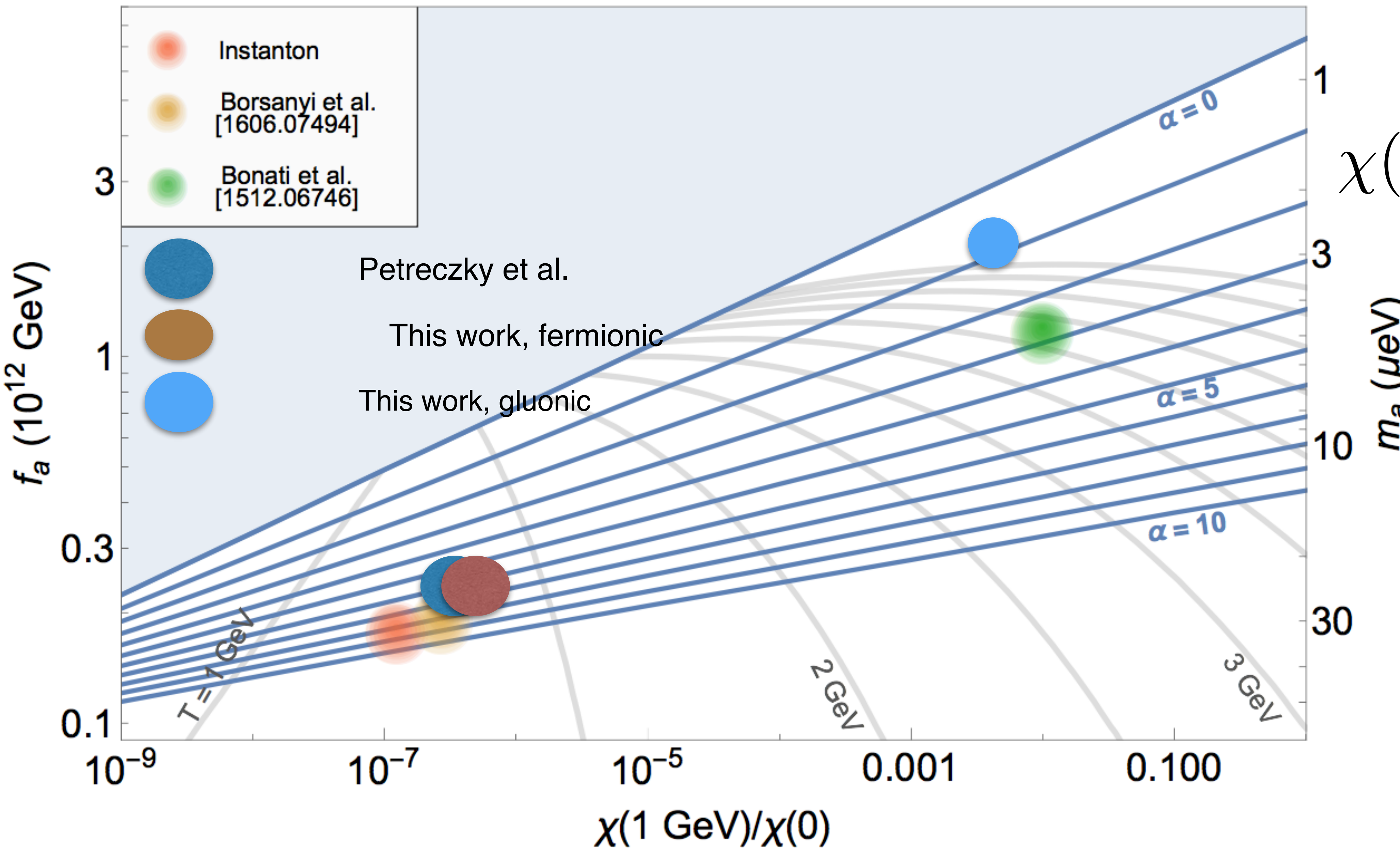

$$\chi(T) \propto 1/T^{\alpha}$$
$$T > 1\ \mathrm{GeV}$$

PhD Thesis, G. Grilli di Cortona, Sissa 2016
(advisor G. Villadoro)

Lower limits on the axion mass assuming that axions make 100% of DM:

Tg: This work, gluonic; Bon: Bonati et al.; D: DIGA, B: Borsanyi et al.,
P: Petreczky et al., T: this work, fermionic

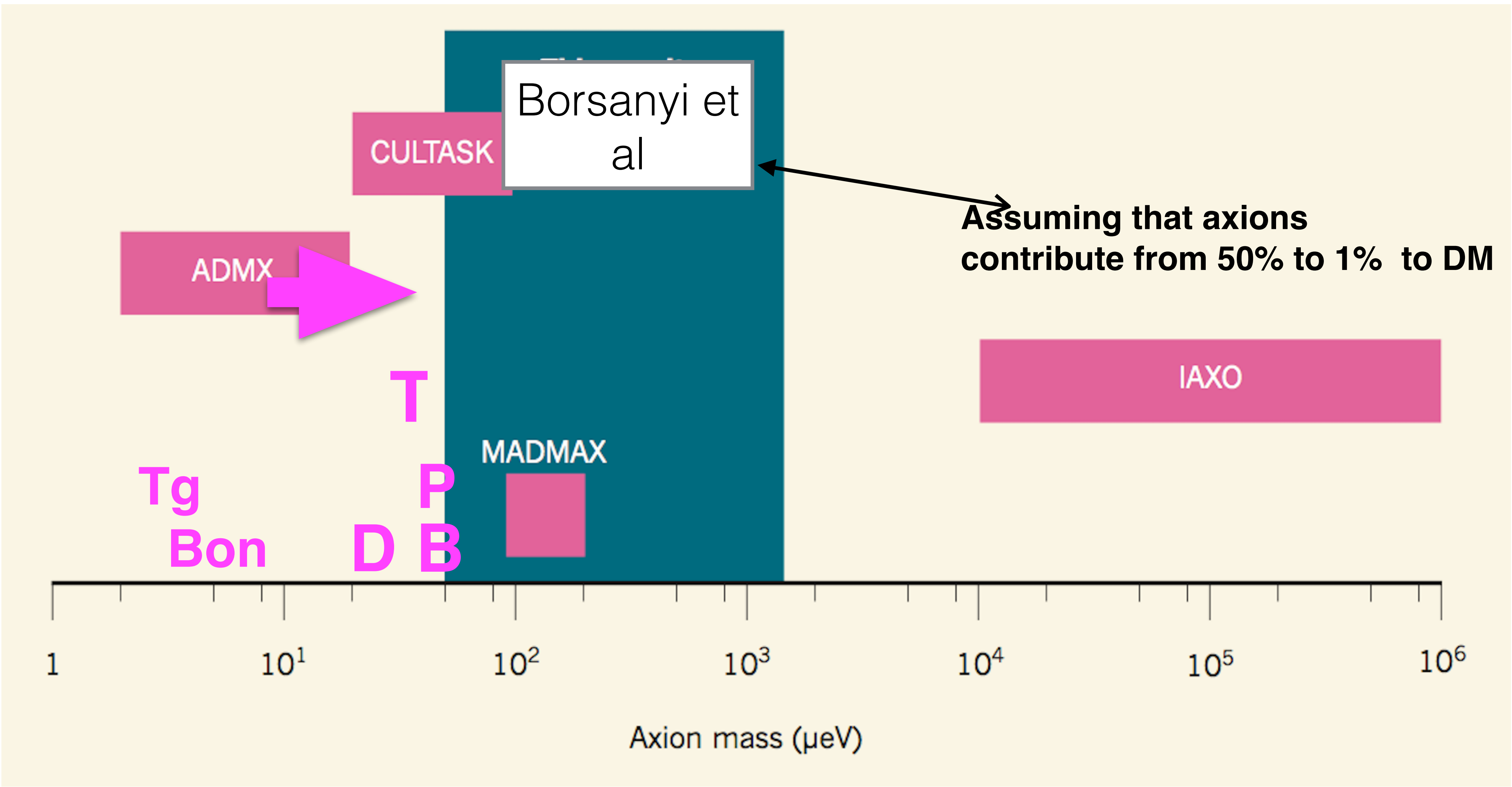

Updated from Nature N&V

Summary

- There is an emerging evidence that the QGP behaves as a DIGA for T > 300 MeV, but such evidence only comes from the exponent and b2. Could this agreement be accidental?

- Differences among different groups/actions should be understood and possibly resolved.

- The behavior around Tc is still under scrutiny, and should be clarified to better understand the approach to DIGA, the nature of the medium produced at the LHC, and the fate of the UA(1) symmetry.

..to get back to hadrons..

PHYSICAL REVIEW D VOLUME 53, NUMBER 9 1 MAY 1996

Return of the prodigal Goldstone boson

J. Kapusta
School of Physics and Astronomy, University of Minnesota, Minneapolis, Minnesota 55455

D. Kharzeev
Theory Division, CERN, Geneva, Switzerland
and Fakultät für Physik, Universtät Bielefeld, Bielefeld, Germany

L. McLerran
School of Physics and Astronomy, University of Minnesota, Minneapolis, Minnesota 55455
(Received 14 July 1995)

We propose that the mass of the η' meson is a particularly sensitive probe of the properties of finite energy density hadronic matter and quark-gluon plasma. We argue that the mass of the η' excitation in hot and dense matter should be small, and, therefore, that the η' production cross section should be much increased relative to that for pp collisions. This may have observable consequences in dilepton and diphoton experiments.

Significant in-medium η' mass reduction in $\sqrt{s_{NN}} = 200$ GeV Au+Au collisions at the BNL Relativistic Heavy Ion Collider

R. Vértesi[1], T. Csörgő[2,1] and J. Sziklai[1]